

Sudan University of Science and Technology



College of Graduate Studies

Design of Solar, Batteries and Diesel Hybrid Power System for Telecommunications Applications

تصميم نظام توليد هجين بين الطاقة الشمسية والبطاريات و الديزل للاستخدام في مجال الاتصالات

A Thesis Submitted in Partial Fulfillment for the Requirements for the Degree of M.Sc. in Electrical Engineering (Power)

Prepared by:

Mohammed Abdlla Mohammed Abdlla

Supervisor:

Dr. Nagmeldeen Abdo Mustafa Hassanain

قال تعالى:

بسم الله الرحمن الرحيم

(قُلْ هَلْ يَسْتَوي الَّذِينَ يَعْلَمُونَ وَالَّذِينَ لا يَعْلَمُونَ إِنَّمَا يَتَذَكَّرُ أُولُو الأَلْبَابِ

صدق الله العظيم

سورة الزمر (الاية 9)

DEDICATION

This thesis is dedicated to the sake of Allah, my creator, and my Master, to my great teacher and messenger Mohammed (May Allah bless and grant him) who taught us the purpose of life.

I am dedicating this thesis to my parents, who have always loved me unconditionally and whose good examples have taught me to work hard for the things that I aspire to achieve.

I am dedicating this thesis to my wife who has been a constant source of support and encouragement during the challenges of life.

I am dedicating this thesis to my brothers, sister and friends for their unlimited assistance in numerous ways.

ACKNOWLEDGMENT

I would like to express my deepest gratitude to my supervisors **Dr. NagmEldeen Abdo** for his support, valuable advice, and guidance throughout this work. He gave a great effort for connection of necessary concepts to complete this search, I extend to him my deepest thanks and appreciation, and ask Allah to bless and guide him.

I extend my thanks to Karim Mohamed from Ericsson for the great support and advice I can never pay you back for all the help you have provided me. There are several people without them this thesis might not have been written, and to them I am greatly indebted.

I would like to take this opportunity to say warm thanks to all my beloved friends, who have been so supportive along the way of doing my thesis. I also would like to express my wholehearted thanks to my family for their generous support they provided me throughout my entire life and particularly through the process of pursuing the master degree. Because of their unconditional love and prayers, I have the chance to complete this thesis.

ABSTRACT

In the world twenty two percent of populations live without electricity. Many of these people live in remote areas where decentralized generation is the only method of electrification. Most mini-grids are powered by diesel generators, but new hybrid power systems are becoming a reliable method to incorporate renewable energy while also reducing total system cost.

The aims of this research were to study and design the hybrid Solar, Batteries and Diesel system applied for Direct Current (DC) telecommunication load to combined different power sources in one system with best performance and efficiency. Most of the existing system works with hybrid diesel-batteries only that had a lot of problems especially with the costly batteries.

In this study Photo Voltaic (PV) module is added with electronic Max Power Point Tracker (MPPT) to the system with site controller that will manage the PV, batteries, and diesel generator to secure the needed power for the critical telecommunication load.

Comparison between hybrid Solar, batteries and Diesel system in term of system design and performance is done using data coming from the real site. The results are compared with the simulation results. The simulation was done by using MATLAB/SIMULINK and the system was divided to five sub systems. The sub systems showing PV system, DC-DC converter system, battery system, Diesel generator and rectifier sub system and the telecommunication load sub system.

Finally, we can say that there was good agreement achieved between the theoretical simulation and the real-time measurement taken from the telecommunication site. We can consider this solution very effective for small scale application not only for telecommunication sites.

مستخلص

يعيش 22 في المئة من سكان العالم بدون كهرباء وكثير من هؤلاء الناس يعيشون في المناطق النائية حيث التوليد اللامركزي للطاقة هو الوسيلة الوحيدة لتوليد الكهرباء . معظم شبكات الطاقة الصغيرة الان تعمل عن طريق مولدات الديزل، ولكن أنظمة الطاقة الهجينة الجديدة أصبحت وسيلة يمكن الاعتماد عليها لدمج الطاقة المتجددة وخفض أيضا التكلفة الإجمالية للنظام.

من اهداف هذا البحث دراسة الطاقات الهجين بين الطاقة الشمسية، البطاريات ونظام الديزل للحصول الطاقة التي تحتاجها اجهزة الاتصالات العاملة بالتيار المباشر وذلك بتجميع مصادر الطاقة المختلفة في نظام واحد لتحقيق أفضل أداء وكفاءة. معظم الانظمة الهجين القائمة الان تعمل بالديزل والبطاريات والتي يوجد بها الكثير من المشاكل خصوصا مع البطاريات المكلفة.

وتهدف الدراسة الي مقارنة الطاقات الهجين كل الطاقة الشمسية، والبطاريات ونظام الديزل من حيث مدة التصميم النظام والأداء من خلال البيانات المأخوذة القادمة من الموقع الحقيقي ومقارنتها مع نتائج المحاكاة. وقد تمت المحاكاة باستخدام ماتلاب وقسم النظام إلى خمسة انظمة فرعية. النظم الفرعية التي تبين نظام الكهروضوئية، ونظام البطارية، ومولد الديزل ومحول التيار المباشر ونظام اجهزة الاتصالات الفرعي.

وأخيرا، يمكننا أن نقول أن هناك اتفاقا جيداً في النتائج التي تحققت بين المحاكاة النظرية وقياس الوقت الحقيقي المأخوذة من موقع الاتصالات. يمكن أن نعتبر هذا الحل فعال جدا للتطبيق على نطاق صغير ليس فقط لمواقع الاتصالات.

TABLE OF CONTENTS

	Page
ועבַּ	i
DEDICATION	ii
ACKNOWLEDGMENT	iii
ABSTRACT	iv
المستخلص	v
LIST OF FIGURES.	vii
LIST OF TABLES.	X
LIST OF ABBREVIATIONS	xi
CHAPTER ONE	
INTRODUCTION 1.1General Concepts	1
1.2 Problem Statement	
1.3 Objectives	
1.4 Methodology	
1.5 Thesis Layout	
CHAPTER TWO	
BACKGROUND AND LITERATURE REVIEW	
2.1 Introduction.	5
2.2 Solar Energy.	5
2.3 Photovoltaic Cells and Efficiencies	6
2.4 The Mathematical Modeling of Solar Cell, Module and Array	9
2.4.1 The solar cell	9
2.4.2 PV module and array	10
2.5 Batteries.	11
2.5.1 Types of batteries	13
2.5.2 The lead acid battery	13
2.5.3 Battery model	15
2.6 Pervious Work	17

CHAPTER THREE

DESIGN OF THE HYBRID POWER S	SYSTEM
-------------------------------------	--------

3.1 Introduction.	27
3.2 PBC 05 HC Solar Hybrid	27
3.3 Solar Panels	32
3.4 Panel Support Structure	34
3.5 Exide OPzS Batteries	35
3.6 OPzS Battery Boxes	36
3.7 Diesel Generator	38
3.8 The Site Design and Consideration	40
3.9 Summary	43
CHAPTER FOUR	
SYSTEM MODELING AND SIMULATION RESULTS	
4.1 Introduction	44
4.2 Simulink Model Construction of PV System	44
4.3 Simulink Model Construction of Buck DC-DC Converter	46
4.4 Simulink Model for Battery System	50
4.5 Simulink Model for DG, Rectifier, and Telecommuncation load systematical systems and the systems of the system of the systems of the system of	m.52
4.6 Simulation Results	53
4.6.1 PV system output voltage	54
4.6.2 PV system output current	55
4.6.3 DC-DC converter output voltage and current	56
4.6.4 The load output voltage and Current	57
4.6.5 The battery voltage, current and SOC	58
CHAPTER FIVE	
CONCLUSION AND RECOMMENDATIONS	
5.1 Conclusion	
5.2 Recommendations	63
REFERENCES	64

LIST OF FIGURES

Figure	Title	Page
2.1	Solar cell diagram	
2.2	General equivalent circuit of PV cell	9
2.3	a) P-V curve for the PV module at 1000W/m² and 554.5W/m² (b) I-V	
	curve for the PV module at 1000W/m² and 554.5W/m²	
2.4	PV cell, module, and array	12
2.5	General equivalent circuit of PV module	12
2.6	Thevenin battery model	16
2.7	Modified Thevenin equivalent circuit model	16
2.8	Solar PV/Mains/Diesel (SMD) Hybrid UPS system	24
3.1	Schematic drawing for the hybrid PV and diesel with backup battery	28
3.2	PBC 05 HC solar hybrid DC power system	29
3.3	Mono-crystalline solar panel	34
3.4	Solar structure's overview	35
3.5	Exide's OPzS solar batteries	36
3.6	Battery Box's overview	42
3.7	Plan view for the solar panels configuration	42
4.1	Solar-diesel hybrid power system with back up batteries applied for	44
	telecom load Simulink model	
4.2	Equivalent circuit for the Solar Cell	45
4.3	PV system Simulink model	46
4.4	Buck converter circuit diagram	47
4.5	Buck converter circuit when switch s is on (Mode-I)	47
4.6	Buck converter circuit when switch s is off (Mode-II)	48
4.7	Supply current Is, diode current ID, inductor current I, and Inductor	49
	Voltage V_L waveforms respectively (Buck Converter)	
4.8	Buck converter Simulink model	50
4.9	Battery discharge characteristics	50
4.10	Battery state of charge characteristics	51
4.11	Battery system Simulink model	51
4.12	Battery system parameters values	52
4.13	Simulink model for the DG and rectifier system	52

4.14	DG and rectifier control system flow chart		
4.15	Simulink model for the telecom load	53	
4.16	The hybrid sites monitoring system GUI	54	
4.17	The monitoring system PV output voltage	55	
4.18	Simulation for PV system output voltage	55	
4.19	Simulation for PV system output current	56	
4.20	Simulation for DC-DC converter output voltage	56	
4.21	Simulation for DC-DC converter output current	57	
4.22	Simulation for the load output voltage	58	
4.23	Simulation for the load output current	58	
4.24	The monitoring system battery voltage	59	
4.25	Simulation for the battery voltage	59	
4.26	The monitoring system battery current	60	
4.27	Simulation for the battery current	60	
4.28	The monitoring system battery sate of charge	61	
4.29	Simulation for the battery state of charge	61	

LIST OF TABLES

Table	Title		
2.1	Common rechargeable battery types		
3.1	PBC 05 HC solar hybrid's mechanical characteristics	29	
3.2	PBC 05 HC solar hybrid's Environmental characteristics	29	
3.3	PBC 05 HC solar hybrid's AC input characteristics	30	
3.4	PBC 05 HC solar hybrid's DC input characteristics	30	
3.5	PBC 05 HC solar hybrid's DC output characteristics	31	
3.6	Solar panel's electrical characteristics	32	
3.7	Solar panel's mechanical characteristics	33	
3.8	Solar panel's different temperature ratings and coefficients	33	
3.9	F4L2011's engine details	38	
3.10	PI144G's technical details	39	
3.11	Monthly average solar insolation values	40	
3.12	Different discharging rates of OPzS solar batteries	41	

LIST OF ABBREVIATIONS

DC Direct Current

PV Photo Voltaic

DG Diesel Generator

KWh Kilowatt Hour

SOC State of Charge

NiCd Nickel Cadmium

NiMH Nickel-Metal Hydride

SLA Small Sealed Lead Acid

VRLA Valve Regulated Lead Acid

DAC Direct Air Cooling

NREL National Renewable Energy Laboratory

MPPT Max Power Point Tracker

PV Photo Voltaic

CHAPTER ONE

INTRODUCTION

1.1 General Concepts

The world's resources of fossil fuels are beginning to come to an end. Estimates of energy resources vary but oil and gas reserves are thought to come to an end in roughly 40 and 60 years respectively and coal reserves could only be able to last another 200 years. The rapid depletion of fossil fuel resources on a worldwide basis has necessitated an urgent search for alternative energy sources to cater to the present days' demand. Environments also are reason to reduce our reliance on fossil fuels because growing evidence of the global warming phenomena. Since the industrial revolution, by burning these fossil fuels, we have caused a dramatic increase in the release of carbon dioxide into the atmosphere. The carbon dioxide gathers in the atmosphere and soaks up the long-wave, infrared radiation reemitted from the earth that would normally be released into space. By keeping this radiation in the earth's atmosphere, it has caused a rise in the earth's temperature. This global warming effect will have far reaching consequences if it is not minimized as soon as possible. The earth's natural balance is very delicate and a rise in temperature even by 1°C or 2°C can melt the ice caps causing wide spread flooding across the world [1].

Therefore, it is imperative to find alternative energy sources to cover the continuously increasing demand of energy while minimize the negative environmental impacts. The option of alternative energy resources such as solar, wind, biomass, ocean, thermal and tidal has attracted energy sectors to generate power in a large scale. The sun is a source of practically unlimited energy, most of which is wasted but provides us with millions of kilowatts of power, keeps us warm, and grows all our food. Every day the sun showers Earth with several thousand times as much energy as we use. To top it off,

solar energy is safe, pollution-free energy on and in which living things have thrived since they first appeared on earth.

The history of solar energy is as old as humankind. In the last two centuries, we started using Sun's energy directly to generate electricity. In 1839, French physicist Alexandre Edmond Becquerel discovered that certain materials produced small amounts of electric current when exposed to light.

It was not utilized until 1946 that the photovoltaic cells were patented by a man named Sven Ason Berglund. 1954 has been declared the modern age of solar technology. This happened when the Bell Laboratories, while experimenting with semiconductors, discovered that the use of silicon could be extremely effective. It was a complete breakthrough. Silicon set to function with certain impurities was actually extremely sensitive to light. The 1954 breakthrough of the Bell Laboratories caused certain solar energy devices to be effective up to 6% ~ but it does not stop there. Following this incredible break through the amount of interest in solar energy and generating solar power from solar cells increased dramatically. Suddenly, the research and discovery of new and more modern solar power apparatuses were being heavily sponsored and believed in. In 1956, solar photovoltaic cells were far from economically practical. Electricity from solar cells ran about \$300 per watt (For comparison, current market rates for a watt of solar PV hover around \$5). The "Space Race" of the 1950s and 60s gave modest opportunity for progress in solar, as satellites and crafts used solar panels for electricity generation. It was not until 1973 that solar leapt to prominence in energy research. The Oil Crisis demonstrated the degree to which the Western economy depended upon a cheap and reliable flow of oil. As oil prices nearly doubled over night, leaders became desperate to find a means to reduce this dependence. The hope in the 1970s was that, through massive investment in research, solar photovoltaic costs could drop precipitously and eventually become competitive with fossil fuels. By the 1990s, the reality was that costs

of solar energy had dropped as predicted, but costs of fossil fuels had also dropped - solar was competing with a falling baseline.

However, huge PV market growth in Japan and Germany from the 1990s to the present has reenergized the solar industry. In 2002 Japan installed 25,000 solar rooftops. Such large PV orders are creating economies of scale, thus steadily lowering costs. The PV market is currently growing at a blistering 30 percent per year, with the promise of continually decreasing costs [2].

1.2 Problem Statement

Unavailability of the Gird power is becoming the biggest problem for developing the rural area specially the areas where there are access roads problems.

The telecommunication service is becoming the most important service for all people and the telecommunication company must be shore that they are delivering the best service all the time. All the telecommunication operators are investing to secure the needed power to run the sites in the rural areas specially the solar and hybrid application, so due that the solar and hybrid system becoming very important subject for research.

1.3 Objectives

The main objectives for this thesis are:

- 1. To assess the Off-Grid PV, batteries and diesel hybrid scenario for telecommunication load in the rural areas, by studying the site design and performance data.
- 2. Validate the system efficiency and to quantify fuel cost savings created by the hybrid system.

1.4 Methodology

To achieve the objectives of the research the methodology is divided into several tasks as follow:

- ➤ Building a strong background about the hybrid system especially the solar and diesel, so I started my thesis with the literature survey of hybrid system, with the focus on the PV, batteries and diesel generator.
- Assessment of Solar/ Solar Diesel Hybrid for off Grids applications elsewhere in the world by utilizing the literature on the internet and various publications at the library.
- ➤ Collecting all the data about the site selected for the study and consider the minimum requirements and the site owner requirements.
- ➤ Build simulation model for the system using Matlab application considering the design data from the site under study.
- ➤ Analyzing and validation for the results obtained during the research period.

1.5 Thesis Layout:

There are five chapters in this thesis including the current chapter as Introduction. Chapter two presents backgrounds about photovoltaic energy conversions and shows all the system components and literature review for the different studies. Chapter three focus on the design of site under study and the real components for the system. Chapter four details out the modeling and simulation part for the system also present simulation results and discussion, in chapter five concludes the thesis.

CHAPTER TWO

BACKGROUND AND LITERATURE REVIEW

2.1 Introduction

In this chapter, we will discuss the dynamic behavior of the photovoltaic (PV) system and discusses the nonlinearity of PV output characteristics. First, it summarizes the commercial solar cells used in PV module. Second, it shows the operational mechanism for crystalline silicon solar cell. Third, it describes the mathematical modelling for solar cell, module and array. Fourth, it emphasis how to intensify the electricity generated from the solar panels. Finally, the pervious works are presented.

2.2 Solar Energy

The sun is the original source of almost all the energy used on earth. The earth receives a stock ring amount of energy from the sun, as much energy falls on the planet each hour is the total human's population uses in a whole year. Photovoltaic technology enables the creation of electricity using light. PV cells have at least two layers of semiconductors: one that's positively charged, and one that's negatively charged. When the light shines on the semiconductor the electric field across the junction between these two layers causes electricity to flow. The greater the intensity of light the stronger the electricity flow will be.

The light that hits the panels is converted into clean electricity. This is a silent operation here because there are no moving parts. The electricity generated by the panels comes in the form of a direct current. By installing an inverter, it is converted into alternating current, so it's in synchronous with the mains electricity and can be used normally. The clean electricity is then fed into the mains by the fuse board. By using meters, the amount of unused electricity generated can be measured and recorded; any spare electricity can be sold back to the electricity supplier. Country with a wet and cloudy climate, 800kWh/m2 is enough energy to power an energy efficient home. Only 10m2

of PV is needed to provide enough electricity to power such a home entirely from solar energy. Therefore, solar photovoltaic provide a simple and practical way for powering buildings with clean energy.

2.3 Photovoltaic Cells and Efficiencies

The performance of a solar cell is measured in terms of its efficiency in turning sunlight into electricity. Improving solar cell efficiencies while holding down the cost per cell remains one rather important goal of the PV industry. PV cells are generally made either from crystalline silicon, thin film, or from other types of technology as shown below.

1) The Crystalline Silicon Technology (CST):

Crystalline silicon cells are made from thin slices cut from a single crystal of silicon (monocrystalline) or from a block of silicon crystals (polycrystalline). CST is the most common technology representing about 90% of the market today. Its efficiency ranges between 14% and 22%.

Two main types of crystalline cells can be distinguished:

- Monocrystalline (Mono c-Si)
- Polycrystalline (or Multicrystalline) (multi c-Si)

2) Thin film technology:

Thin film modules are made by depositing extremely thin layers of photosensitive materials onto a low-cost backing such as stainless steel, glass or plastic. Thin Film manufacturing processes result in lower production costs compared to the more material-intensive crystalline technology. Such price advantage is counterbalanced by lower efficiency rates (7.3%-10.6%). However, this is an average value and not all Thin Film technologies have the same efficiency.

Four types of thin film modules are commercially available at the moment

- Amorphous Silicon (a-Si)
- Cadmium Telluride (CdTe)

- Copper Indium Selenide, Copper Indium Gallium diSelenide (CIS, CIGS)
- Multi Junction Cells (a-Si/μc-Si)

3) Other cell types:

Several other types of more recently developed photovoltaic technologies have been commercialized or are still at the research level. The main ones are:

- Concentrated photovoltaic: it is solar cells that are designed to operate
 with concentrated sunlight. They are built into concentrated collectors
 that use a lens to focus the sunlight onto the cells. The main idea is to
 use very little of the expensive semiconducting PV material while still
 collecting as much sunlight as possible.
- Flexible cells: based on a similar production process to thin film cells, when the active material is deposited in a thin plastic, the cell can be flexible. This opens the range of applications, especially for building integration (roofs-tiles) and end-consumer applications.

The cells efficiency decreases with increases in the temperature. Crystalline cells are more sensitive to heat than thin films cells. The output of a crystalline cell decreases approximately 0.5% with every increase of one degree Celsius in cell temperature. For this reason, modules should be kept as cool as practically possible. For this reason, amorphous silicon cells may be preferred in very hot conditions because their output decreases by approximately 0.2% per degree Celsius increase.

As the crystalline silicon cells is the most used type of PV and also we are considering it for this research the will be studding it in more details than the others types. Figure 2.1 shows the operation of the silicon solar cell. It can be seen that when light strikes the cell, a certain portion of the light's energy is absorbed within the semiconductor material. The energy knocks electrons loose, allowing electrons to flow freely. The PV cells have one or more electric fields that act to force the electrons freed by light absorption to flow in a certain direction. The P-type silicon ("p" for positive) has free holes

which are just the absence of electrons. The N-type silicon ("n" for negative) has free electrons.

P-N junction is created when a p-type semiconductor is joined to an n-type semiconductor. Diffusion current is produced due to the concentration differences of holes and free electrons between the n- and p- regions: electrons flow from the n-side and fill holes on the p-side. This creates a region that is almost devoid of free charge carriers (i.e. free electrons or holes) and is therefore called the depletion layer.

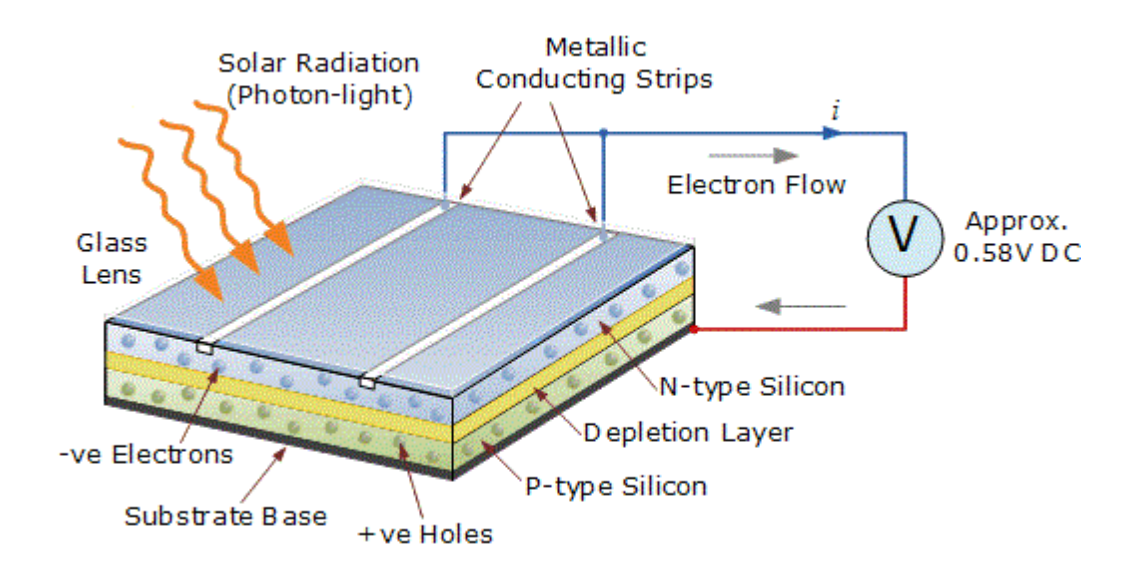


Figure 2.1: Solar cell diagram

There is in the depleted zone a net positive charge on the n-side and a net negative charge on the p-side in the depleted zone. Such situation results in an electric field that opposes any further flow of electrons. The more electrons move from the n-to the p-side, the stronger the opposing field will be, and eventually equilibrium will be reached in which no further electrons are able to move against the electric field.

The equilibrium conditions are disturbed when light hits the solar cell and the so-called inner photo effect creates additional charge carriers that are free to move in the electric field of the depletion zone. The holes move towards the p-region and the electrons towards the n-region, thus creating an external

voltage at the cell. This external voltage in a solar cell is material dependent and does not depend on the cell's surface area.

2.4 The Mathematical Modeling of Solar Cell, Module and Array

A simple equivalent circuit model for the photovoltaic cell consist of a real diode in parallel with an ideal current source as shown in Figure 2.2. The solar cell is basically a p-n junction fabricated in a thin wafer or a layer of semiconductor. The electromagnetic radiation of solar energy can be directly converted into electricity through the photovoltaic effect. When exposed to sunlight, photons with energy greater than the band-gap energy of the semiconductor are absorbed and they create some electron-hole pairs proportional to the incident irradiation. Under the influence of the internal electric fields of the p-n junction, these carriers are swept apart and they create a photocurrent which is directly proportional to solar insulation. The PV system naturally exhibits a nonlinear I-V and P-V characteristics which vary according to the solar irradiance and cell temperature.

2.4.1 The solar cell

As mention above the circuit of the solar cell model is consist of a real diode in parallel with an ideal current source, in addition the model will be more accurate by adding in parallel resistor (leakage current) and a series resistor.

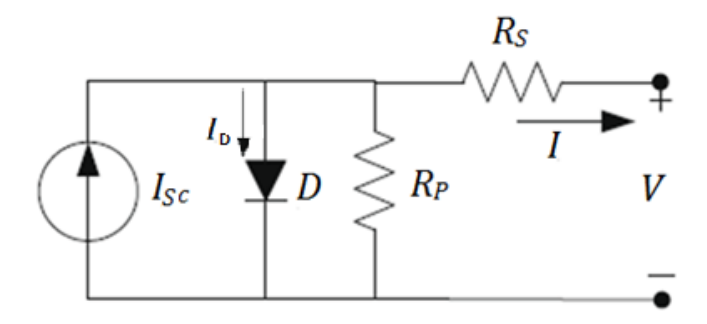


Figure 2.2: General equivalent circuit of PV cell

The power output current for the solar cell is given by:

$$I = I_{sc} - I_d = I_{sc} - I_o \left(e^{q V_d / KT} - 1 \right) \tag{2.1}$$

Adding R_s impact

$$V_d = V + I.R_s \tag{2.2}$$

This will give

$$I = I_{sc} - I_{\circ} \{ \exp[q(V + I.R_s)/KT] - 1 \}$$
(2.3)

To generalize the PV equivalent circuit by including both series and parallel resistances.

$$I = I_{sc} - I_{\circ} \left\{ \exp[q(V + I.R_s)/KT] - 1 \right\} - \left(\frac{V + I.R_s}{R_P}\right)$$
 (2.4)

Where:

 I_{sc} is the light generated current.

 I_{\circ} is the saturation current dependent on the cell temperature.

q is the electric charge (1.6 x 10-19 C).

K is the Boltzmann's constant $(1.38 \times 10^{-23} \text{ J/K})$.

T is the cell's absolute temperature.

 R_s is the series resistance.

 R_P is the parallel resistance.

2.4.2 PV module and array

The output power of the solar cell is said to reach approximately 2W at 0.5V. Figure 2.3 below is showing the P-V and I-V Curves for modules at 1000W/m² and 554.5W/m². To increase the power, the cells are connected in

series-parallel configuration on a module. For photovoltaic systems, the PV array is the group of several PV modules which are connected in series and parallel circuits to generate the required voltage and current. Figure 2.4 shows this configuration the equivalent circuit for the solar module arranged in NP parallel and NS series branches is shown in Figure 2.5.

The terminal equation for the current and voltage of the cell module comes out as follows:

$$I = N_p I_{sc} - N_p I_{\circ} \left\{ \exp\left[q\left(\frac{V}{N_s} + I \frac{R_s}{N_P}\right) / KT\right] - 1\right\} - \left(\frac{N_p}{N_s}\right)$$
 (2.5)

Where:

 N_s is the number of cells in series.

 N_p is the number of cells in parallel.

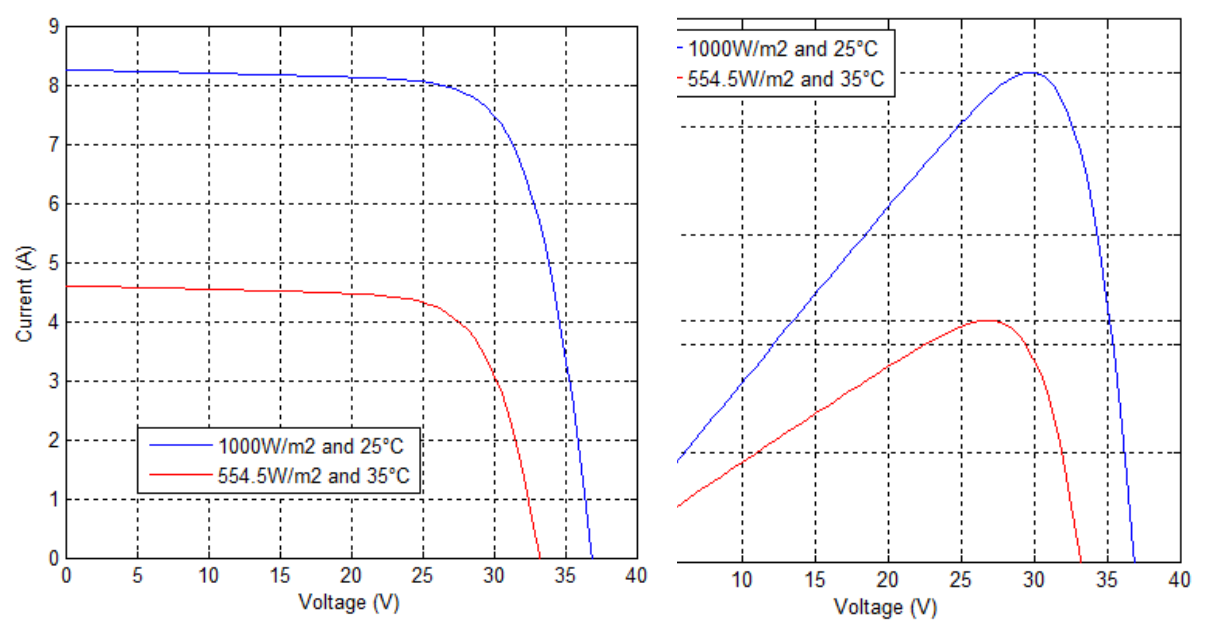


Figure 2.3: (a) P-V curve for the PV module at 1000W/m² and 554.5W/m² (b) I-V curve for the PV module at 1000W/m² and 554.5W/m²

2.5 Batteries

A battery is a device that converts chemical energy directly to electrical energy. It contains one or more cells. Each cell consists of three main parts: a positive electrode (terminal), a negative electrode, and a liquid or solid

separating them called the electrolyte. When a battery is connected to an electric circuit, a chemical reaction takes place in the electrolyte causing ions (in this case, atom with a positive electrical charge) to flow through it one way. With electrons (particles with a negative charge) flowing through the

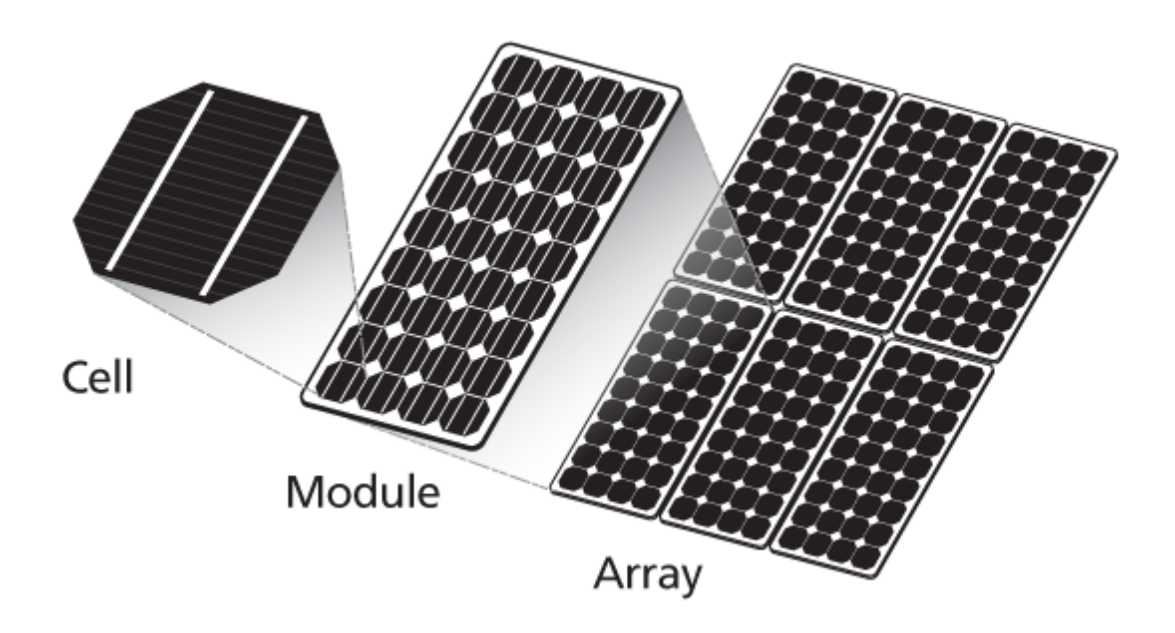


Figure 2.4: PV cell, module, and array

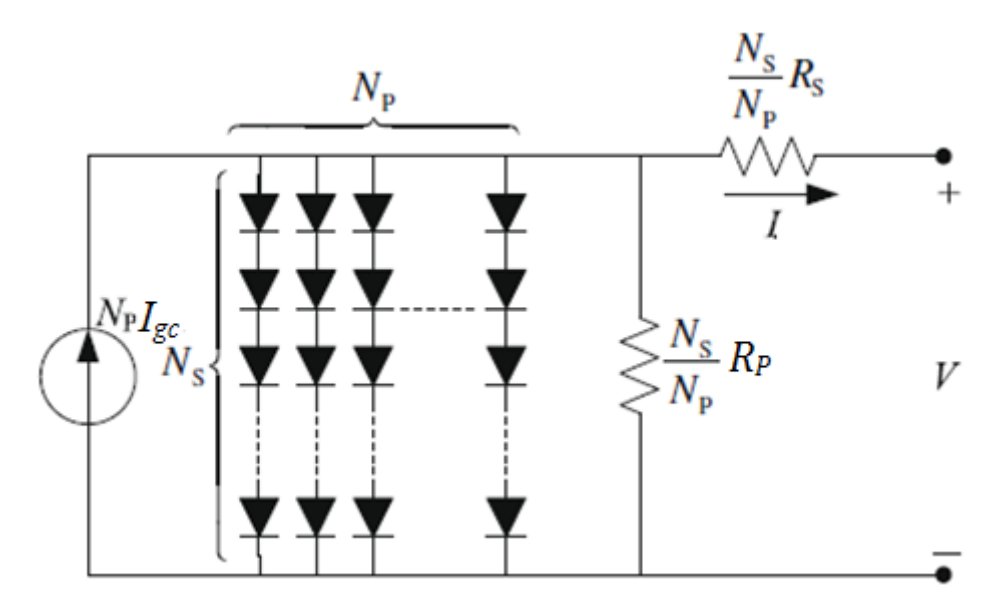


Figure 2.5: General equivalent circuit of PV module

outer circuit in the other direction. This movement of electric charge makes an electric current flow through the cell and through the circuit it is connected to (Dell and Rand 2001). Different types of batteries are produced for

different applications. They can be used for storing solar power for satellites in space to powering heart pacemakers fitted inside people's chests.

2.5.1 Types of batteries

There are two types of batteries:

- Primary batteries (disposable batteries): which are designed to be used once and discarded.
- Secondary batteries (rechargeable batteries): which are designed to be recharged and used multiple times.

Most of the batteries used today with hybrid power system are from the rechargeable type. There are several kinds of rechargeable batteries. Among them, as shown in Table 5.1: NiCd (Nickel Cadmium), NiMH (Nickel Metal Hydride), Lead-Acid, and Lithium-Ion (Li-Ion).

Table 2.1: Common rechargeable battery types

Parameters	NiCd	NiMH	Lead-Acid	Lithium-Ion
Nominal cell voltage (V)	1.25	1.25	2	3.6
Energy density (Wh/kg)	45-80	60-120	30-50	110-160
Specific power (W/kg)	150	250-1000	180	1800
Self-discharge rate in (%/month)	20%	30%	3%-4%	5%-10%
Cycle durability ₃ (#)	1500	300-500	200-300	500-1000
Charge/discharge efficiency (%)	70%-90%	66%	70%-92%	99%+
Maintenance Requirement	30 to 60 days	60 to 90 days	3 to 6 months9	not req.
Typical Battery Cost	\$50	\$60	\$25	\$100
(US\$, reference only)	(7.2V)	(7.2V)	(6V)	(7.2V)
Cost per Cycle(US\$)11	\$0.04	\$0.12	\$0.10	\$0.29

2.5.2 The lead acid battery

Invented by the French physician Gaston Planté in 1859, lead acid was the first rechargeable battery for commercial use. Today, the flooded lead acid battery is used in automobiles, forklifts and large uninterruptible power supply (UPS) systems. During the mid 1970s, researchers developed a

maintenance-free lead acid battery that could operate in any position. The liquid electrolyte was transformed into moistened separators and the enclosure was sealed. Safety valves were added to allow venting of gas during charge and discharge. Driven by different applications, two battery designations emerged. They are the small sealed lead acid (SLA), also known under the brand name of Gel cell, and the large valve regulated lead acid (VRLA). Technically, both batteries are the same. (Engineers may argue that the word 'sealed lead acid' is a misnomer because no lead acid battery can be totally sealed). Unlike the flooded lead acid battery, both the SLA and VRLA are designed with a low over-voltage potential to prohibit the battery from reaching its gas-generating potential during charge. Excess charging would cause gassing and water depletion. Consequently, these batteries can never be charged to their full potential. The lead acid is not subject to memory. Leaving the battery on float charge for a prolonged time does not cause damage. The battery's charge retention is best among rechargeable batteries. Whereas the NiCd self-discharges approximately 40 percent of its stored energy in three months, the SLA self-discharges the same amount in one year. The SLA is relatively inexpensive to purchase but the operational costs can be more expensive than the NiCd if full cycles are required on a repetitive basis. The SLA does not lend itself to fast charging — typical charge times are 8 to 16 hours. The SLA must always be stored in a charged state. Leaving the battery in a discharged condition causes sulfation, a condition that makes the battery difficult, if not impossible, to recharge. Unlike the NiCd, the SLA does not like deep cycling. A full discharge causes extra strain and each cycle robs the battery of a small amount of capacity. This wear-down characteristic also applies to other battery chemistries in varying degrees. To prevent the battery from being stressed through repetitive deep discharge, a larger SLA battery is recommended. Depending on the depth of discharge and operating temperature, the SLA provides 200 to 300 discharge/ charge cycles. The primary reason for its relatively short cycle life is grid corrosion of the positive electrode, depletion of the active material and expansion of the positive plates. These changes are most prevalent at higher operating temperatures. Cycling does not prevent or reverse the trend. The optimum operating temperature for the SLA and VRLA battery is 25°C (77°F). As a rule of thumb, every 8°C (15°F) rise in temperature will cut the battery life in half. VRLA that would last for 10 years at 25°C will only be good for 5 years if operated at 33°C (95°F). The same battery would endure a little more than one year at a temperature of 42°C (107°F). Among modern rechargeable batteries, the lead acid battery family has the lowest energy density, making it unsuitable for handheld devices that demand compact size. In addition, performance at low temperatures is poor.

The SLA is rated at a 5-hour discharge or 0.2C. Some batteries are even rated at a slow 20-hour discharge. Longer discharge times produce higher capacity readings. The SLA performs well on high pulse currents. During these pulses, discharge rates well in excess of 1C can be drawn. In terms of disposal, the SLA is less harmful than the NiCd battery but the high lead content makes the SLA environmentally unfriendly.

2.5.3 Battery model

Thevenin battery model is commonly used model which was designed to account for transient behavior of the battery. The model is shown in the figure 2.6 The R_{\circ} parameter represents the resistance between the contact plates and electrolyte while the C_{\circ} relates to the capacitance between the parallel plates. The big disadvantage of the Thevenin model is the assumption of constancy of all the elements, as they all depend on the SoC and other battery characteristics.

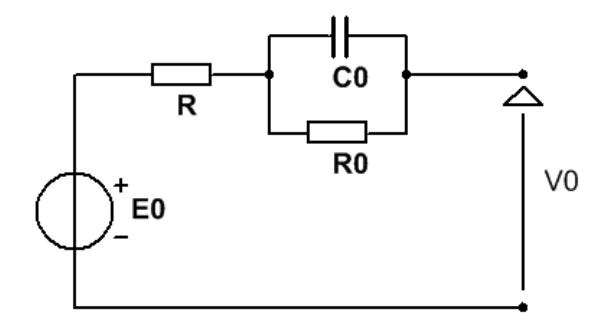


Figure 2.6: Thevenin battery mode

Where:

 E_{\circ} is ideal battery voltage

R is internal resistance

C∘ is capacitance

 R_{\circ} is resistance between the contact plates and electrolyte

The basic Thevenin Battery Model has been improved by Farell as is presented in the figure below.

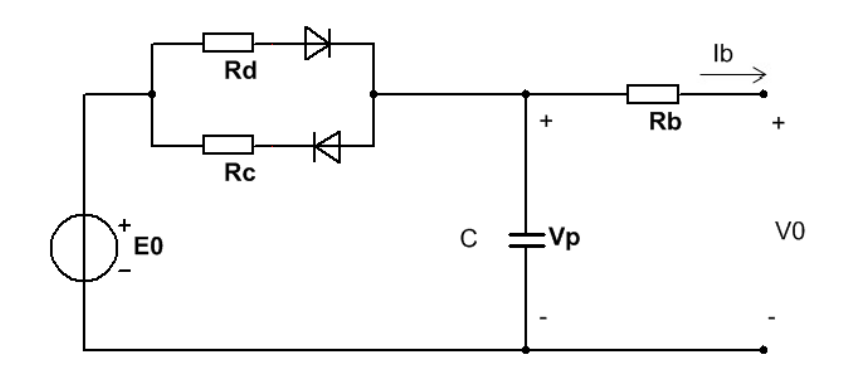


Figure 2.7: Modified Thevenin equivalent circuit model.

The charging/discharging equations are given by

$$\frac{dV_p}{dt} = -V_p \frac{1}{R_d C} + V_0 \frac{1}{R_d C} - I_b \frac{1}{C}, \quad V_p \le V_0
\frac{dV_p}{dt} = -V_p \frac{1}{R_c C} + V_0 \frac{1}{R_c C} - I_b \frac{1}{C}, \quad V_p > V_0$$
(2.6)

2.6 Pervious Work

Hybrid power describes the combination of a power producer and the means to store that power in an energy storage medium. In power engineering, the term 'hybrid' describes a combined power and energy storage system. Examples of power producers used in hybrid power are photovoltaic, wind turbines, generators that use fuel and examples of energy storage media are batteries or hydrogen (for later use in fuel cells).

Hybrid Renewable Energy Systems (HRES) are becoming popular as stand-alone power systems for providing electricity in remote areas due to advances in renewable energy technologies and subsequent rise in prices of petroleum products. A hybrid energy system, or hybrid power, usually consists of two or more renewable energy sources used together to provide increased system efficiency as well as greater balance in energy supply. Research on hybrid power systems combining renewable and fossil derived electricity started 25 years ago, but few have written papers about system implementation and experimental data collection. The first papers describing renewable energy hybrid systems appeared in the mid-eighties [3], but literature on hybrid systems did not blossom until the early 1990s. Initially, this expansion in hybrid literature was driven by the need to increase grid stability and reliability as large quantities of wind power were being added to small autonomous grids [4].

As solar energy is fluctuating, and the generation capacity of the diesel gensets is limited to a certain range, it is often a viable option to include battery storage in order to optimize solar's contribution to the overall generation of the hybrid system. In 2015, a case-study conducted in seven countries concluded that in all cases generating costs can be reduced by hybridizing mini-grids and isolated grids. However, financing costs for diesel-powered electricity grids with solar photovoltaics are crucial and largely depend on the ownership structure of the power plant. While cost reductions for state-owned utilities can be significant, the study also identified economic

benefits to be insignificant or even negative for non-public utilities, such as independent power producers. Other solar hybrids include solar-wind systems. The combination of wind and solar PV has the advantage that the two sources complement each other because the peak operating times for each system occur at different times of the day and year. The power generation of such a hybrid system is therefore more constant and fluctuates less than each of the two component subsystems[5].

Solar hybrid power systems are hybrid power systems that combine solar power from a photovoltaic system with another power generating energy source. A common type is a photovoltaic diesel hybrid system, combining photovoltaics (PV) and diesel generators, or diesel gensets, as PV has hardly any marginal cost and is treated with priority on the grid. The diesel gensets are used to constantly fill in the gap between the present load and the actual generated power by the PV system. To improve the efficiency of the system furthers either cogeneration or tri-generation, can be used. Researches on photovoltaic diesel hybrid system are few papers compared with solar-wind hybrid systems this Chapter presents a literature review on the hybrid system by several aspects: solar and diesel generator energy application potential analysis; PV array, also hybrid wind-solar system turbine and battery performance predictions; optimal sizing method for hybrid solar-wind system; and the optimal sizing method for designing hybrid solar-wind-diesel systems which has combined a third energy source - diesel generator.

The techniques to design and analyze a hybrid wind-solar power system for either autonomous or grid-linked applications. This technique uses linear programming principles to reduce the cost of electricity while meeting the load requirements in a reliable manner. A controller that monitors the operation of the autonomous/grid-linked systems is designed. Such a controller determines the energy available from each of the system components and the environmental credit of the system. It then gives details related to cost, unmet and spilled energies, and battery losses. Until now, a lot

of researches have been done on the analysis of solar and wind energy resources, Among these studies Riad Chedid and Saifur Rahman in 1997 proposed techniques and applied it to a location in Lebanon where the load is defined as 800KW from the 5-th to the 9-th months, and 550KW for the rest of the year. The hourly wind speeds vary between 2.96 and 5.63 m/s and the hourly solar irradiance vary between 0 and 0.7 KW/m2. Results of optimization for both systems shown that it had the load been satisfied only by diesel engines or through a grid connection the required capacity would have been 760 KW.

Therefore, the use of renewable energy has resulted in 50.26% savings in diesel capacity and 44.7% savings in grid capacity. Riad Chedid, H. Akiki and Saifur Rahman in 1998 they continue their research in solar-wind hybrid system and they came with technique for designing hybrid system. When designing HSWPS (hybrid solar-wind power systems), several goals could be aimed at. Examples include reduction in emissions, generation of additional jobs, security of supply, and in some situations, solar and wind resources may constitute the cheapest option for electricity generation. In this paper, the main goal behind proposing HSWPS is to increase the penetration of solar and wind energy technologies in the total energy mix. To achieve this, it is important to highlight all the factors influencing the main goal, whether technical, political, and economical or may be social. Then, a hierarchical structure of the system is built descending from the main goal, down to the constraints, and then down to the policies affecting the constraints, and finally to the outcomes which represent the objectives (attributes).

The various divergences of opinions and influencing factors are identified, weighted and, accordingly, the objectives are assigned a priority order. In the paper three objectives are considered. These are the minimization of both cost and emissions, and the maximization of system reliability [6].

An attempt has been made in this paper to develop a decision support technique which can help decision makers optimally design grid-linked

renewable energy systems. The various procedures of the proposed technique have been fully explained, and a case study on a site in Lebanon has been illustrated. The Analytic Hierarchy Process was used to quantify the various divergences of opinions, practices and events that lead to confusion and uncertainties in planning HSWPS. The application of AHP enforced, on one hand, the cost, reliability and emissions as major design objectives, and on the other hand, ranked them in a priority order. The tradeoff/risk method was used to generate multiple plans under 16 different futures and obtain the corresponding trade-off curves. Unlike the traditional 2-D simulation, a novel modeling of a trade-off surface in 3-D space has been presented where the knee set is determined using the minimum distance approach. Robust and inferior plans are segregated based on their frequent occurrence in the conditional decision set of each future, and since there was no plan which is 100% robust, hedging analysis to reduce risk was performed by assigning alternative options to be adopted in case the risky futures occur. In 2004 S. Arul Daniel and N. Ammasai Gounden prepare study about renewable energy systems based on hybrid wind-solar sources are considered as feasible and reliable options instead of wind-diesel systems. An isolated hybrid scheme employing a simple three-phase square-wave inverter to integrate a photovoltaic array with a wind-driven induction generator has been proposed for the first time. A dynamic mathematical model of the hybrid scheme with variables expressed in – synchronous reference frame has been developed. The model is implemented in the power system block set platform and a comparison has been made between transients simulated and transients experimental obtained in an prototype. Close agreement experimental and the simulated waveforms has been observed, which validates the model [7].

A reliable and simple scheme integrating wind-driven induction generators and PV array has been successfully developed for the first time to supply a three-phase remote load with constant frequency balanced voltages. The

generation system will supply constant voltages with varying wind speed and irradiation when the battery is switched on. The hybrid system is costeffective and requires a simple interface for integration, thus making it suitable for off-grid applications. Lingfeng Wang and Chanan Singh in 2009 prepare paper showing multi source hybrid power generation systems of representative application of the renewables' technology. In this investigation, wind turbine generators, photovoltaic panels, and storage batteries are used to build hybrid generation systems that are optimal in terms of multiple criteria including cost, reliability, and emissions. Multi criteria design facilitates the decision maker to make more rational evaluations. In this study, an improved particle swarm optimization algorithm is developed to derive these nondominated solutions. Hybrid generation systems under different design scenarios are designed based on the proposed approach. First, a grid-linked hybrid system is designed without incorporating system uncertainties. Then, adequacy evaluation is conducted based on probabilistic methods by accounting for equipment failures, time-dependent sources of energy, and stochastic generation/load variations. In particular, due to the unpredictability of wind speed and solar insolation as well as the random load variation, timeseries models are adopted to reflect their stochastic characteristics. An adequacy evaluation procedure including time dependent sources is adopted. Sensitivity studies are also carried out to examine the impacts of different system parameters on the overall design performance [8].

Distributed generation using sustainable clean green power promises to considerably restructure the energy industry that is evolving from fossil fuels toward renewables .Meanwhile, there are many open-ended problems in this field awaiting to be resolved. In this paper, a hybrid power generation system including wind power and solar power is designed on the basis of cost, reliability, and emission criteria. A set of tradeoff solutions is obtained using the multicriteria metaheuristic method that offers many design alternatives to the decision maker. Moreover, in one of the designs, system uncertainties,

such as equipment failures and stochastic generation/load variations, are considered by conducting adequacy evaluation based on probabilistic methods. In particular, the stochastic generation/load variations are modeled through time-series methods. Numerical simulations are used to illustrate the applicability and validity of the proposed MOPSO based optimization procedure, and some sensitivity studies are also carried out. In future studies, other more complicated design scenarios may be incorporated into system designs. In 2012 Toshiro Hirose and Hirofumi Matsuo prepare paper showing the proposes of unique standalone hybrid power generation system, applying advanced power control techniques, fed by four power sources: wind power, solar power, storage battery, and diesel engine generator, and which is not connected to a commercial power system. Considerable effort was put into the development of active-reactive power and dump power controls. The result of laboratory experiments revealed that amplitudes and phases of ac output voltage were well regulated in the proposed hybrid system. Different power sources can be interconnected anywhere on the same power line, leading to flexible system expansion. It is anticipated that this hybrid power generation system, into which natural energy is incorporated, will contribute to global environmental protection on isolated islands and in rural locations without any dependence on commercial power systems. The authors have proposed a unique standalone hybrid wind solar power generation system, which is characterized by PLL control and dump power control. In particular, dump power control allows for formation of a feedback loop in this system, meaning that there is no requirement for a dedicated high-speed line to transmit storage battery voltage and current data.

In case the power line is used as a media for data transmission, the line voltage amplitudes can be applied as a means of data transmission; thus, there is no requirement for installation of any optical fiber transmission line or power line carrier system through which harmonic signals are applied to power line. In addition, neither dump load nor dump load control device are

necessary. Under our dump power control, regulation of output is done without battery overcharging, and effective use of surplus power is made possible. This contributes to battery life extension and realization of a low-cost system. The system, through ac system interconnection, will also allow flexible system expansion in the future. Further, power sources including EG can be flexibly interconnected anywhere through the same power line, and power quality stability can be maintained by controlling the phase and amplitude of ac output voltage. It is expected that this hybrid system into which natural energy is incorporated, and which makes use of various power control techniques, will be applicable in rural locations, even those with poor communications media. The system will also contribute to global environmental protection through application on isolated islands without any dependence on commercial power systems [9].

The hybrid system consists of three power generation systems, photovoltaic arrays, a wind turbine and battery or fuel cell. The PV and wind turbine are used as the main power generation for the system and the battery or fuel cell is assigned as a backup power generator for the continuous power supply.

The design of hybrid power system is mainly dependent on the performance of individual components. In order to predict the system's performance, individual components should be modeled first and then their combination can be evaluated to meet the demand reliability. Over recent years several modelling studies on hybrid renewable energy systems, have been conducted. Among them, Chem V Nayar(1997) Proposed a 10 kVA hybrid uninterrupted power supply system jointly developed by Curtin University and Advanced Energy Systems Ltd in Western Australia and installed in two state capital cities in India with soft loan from the World Bank through the Indian Renewable Energy Development Agency Ltd. The system, incorporating a photovoltaic generator, battery bank, a bi-directional inverter/charger and grid/diesel synchronizing controller, is a fully automatic system which can

provide continuous, conditioned and regulated uninterrupted power for all electrical loads.

The system, shown in Fig below, involves a combination of electrical power sources such as the public electricity grid supply, a battery bank, a stand-by energy source such as a diesel generator and solar photovoltaic generator which produces electricity from sunlight. The system is named as a solar PV/mains/diesel (SMD) Hybrid UPS system and it can provide electrical power for critical functions and equipment when the quality of normal mains power is not adequate or fails entirely.

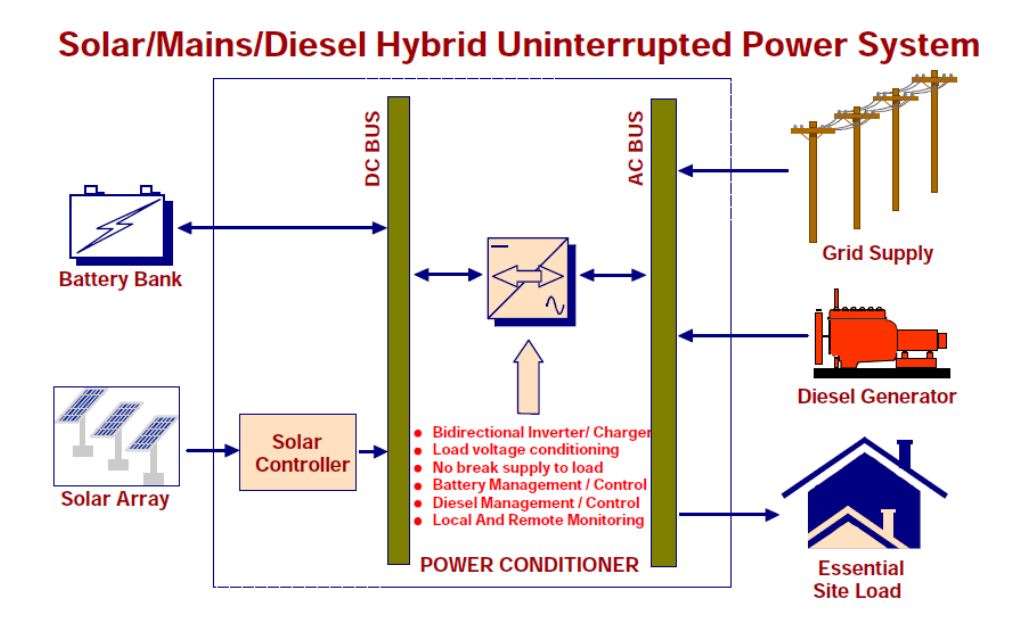


Figure 2.8: Solar PV/Mains/Diesel (SMD) hybrid UPS system

The SMD hybrid system incorporating a bi-directional inverter/charger and grid/diesel synchronizing capability based on well proven Australian power conditioning technology is a fully automatic system which can provide continuous, conditioned and regulated uninterrupted power for all electrical loads. The product is targeted to meet the essential critical loads of consumers such as small offices, business centers, affluent houses, hospitals and educational institutions[10].

In 2013 Xiangjun Li, Dong Hui and Xiaokang Lai prepare paper about the battery energy storage station (BESS) showing the current and typical means of smoothing wind- or solar-power generation fluctuations. Such BESS-based

hybrid power systems require a suitable control strategy that can effectively regulate power output levels and battery state of charge (SOC). This paper presents the results of a wind/photovoltaic (PV)/BESS hybrid power system simulation analysis undertaken to improve the smoothing performance of wind/PV/BESS hybrid power generation and the effectiveness of battery SOC control. A smoothing control method for reducing wind/PV hybrid output power fluctuations and regulating battery SOC under the typical conditions is proposed. A novel real-time BESS-based power allocation method also is proposed. The effectiveness of these methods was verified using MATLAB/SIMULINK software. The disadvantage of PV and wind power generation is their unstable power output, which can impact negatively on utility and micro-grid operations. One means of solving this problem is to integrate PVGS and WPGS with a BESS. For such hybrid generation systems, control strategies for efficient power dispatch need to be developed. Therefore, in this paper, a novel SOC-based control strategy for smoothing the output fluctuation of a WP and PV hybrid generation system has been proposed. Additionally, the SOC feedback control strategy and the real-time power allocation method for timely regulation of battery power and energy are presented. Simulation results demonstrate that the proposed control strategy can manage BESS power and SOC within a specified target region while smoothing PVGS and WPGS outputs.

At present, how to control the SOC of the energy storage system is an ongoing research topic. We also need to combine the characteristics of the battery, and do further research and exploration. From the present research results, it can be seen that by using the proposed control method, the SOC of each battery energy storage unit can gradually move toward 50% with the increase of control time although the initial SOC of the energy storage unit is different. It is also considered that this control method can make the storage unit share the load as consistently as possible, so as to achieve the effect of extending the service life of the energy storage system and, therefore, can

delay the accelerated decay of the battery performance. Moreover, it should be noted that some filtering on the BESS charge and discharge power have been achieved by using a power fluctuation rate constraint as the smoothing control target to prevent excessive excursions to "chase down" every PV or wind power output fluctuation.

In addition, this paper was mainly focused on the control strategies of BESS and smoothing based on battery capacity established conditions. Another significant issue is the means by which an appropriate battery capacity for this application is to be determined. The power control strategies for large-scale wind/PV/BESS hybrid power systems taking into account the optimum capacity of BESS and battery aging will be discussed in the near future combined with smoothing control application of wind and PV power generations [11].

CHAPTER THREE

DESIGN OF THE HYBRID POWER SYSTEM

3.1 Introduction

A "hybrid" is something that is formed by combining two kinds of components that produce the same or similar results. A photovoltaic diesel hybrid system ordinarily consists of a PV system, diesel gensets and intelligent management to ensure that the amount of solar energy fed into the system exactly matches the demand at that time.

The hybrid systems are becoming the best solution for telecom applications because these days all the research is working to reduce the running cost for sites in the rural areas. The rural areas sites are becoming the most expensive due to the fuel transportation cost and limitations in the access roads. This was one of the reasons for this study as we take one of type of the hybrid systems; the system is hybrid PV and diesel with backup battery. The considered site for this study is real telecom site located in Ethiopia and the system was supplied by Ericsson the Sweden vendor as shown in the Figure 3.1, In this chapter, we will show the all the system component and the calculation for the site under our study.

3.2 PBC 05 HC Solar Hybrid

The PBC 05 HC solar hybrid is an outdoor power system which converts input power from AC mains or solar panels into -48V DC power. The PBC 05 solar hybrid DC power system is the most adequate option to be considered when solar hybrid solutions are required as it has both rectifier and solar capabilities. It can support up to 18KW rectifier capacity and 18KW solar capacity.

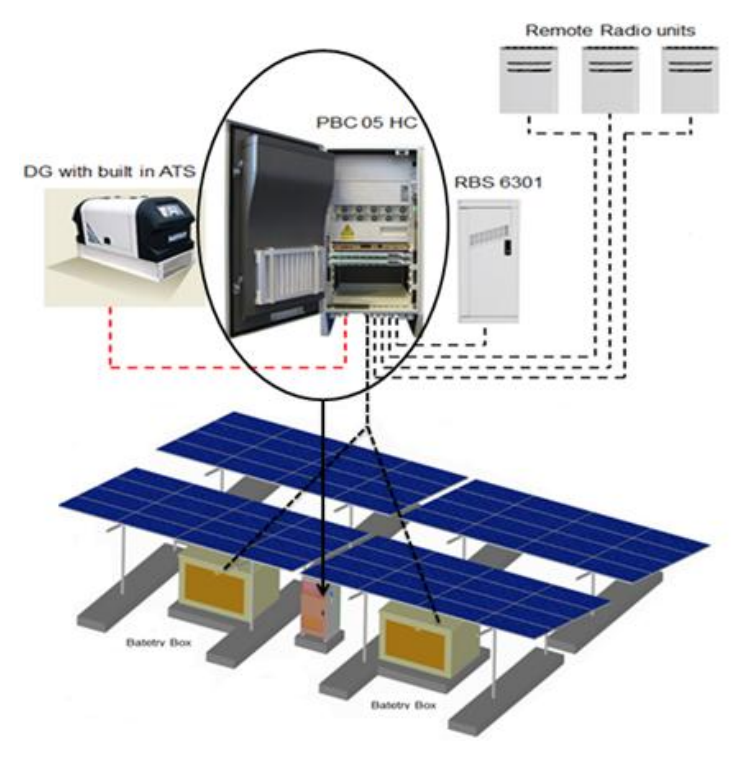


Figure 3.1: Schematic drawing for the hybrid PV and diesel with backup battery

The PBC 05 HC solar hybrid DC power system can be used to power up different Telecom RBS cabinets and remote radio units like RBS 6301, RBS 6102, RBS 6101, RRUS01 and RRUS12. Also, it can be used to power up the different telecom DC equipment after considering the max power. The PBC 05 HC solar hybrid DC power system supports only floor mounting scheme. To ensure long life and low operational cost, the PBC 05 HC solar hybrid features the Direct Air Cooling (DAC) system, with linear speed regulated fans and a particle filter. The temperature is sensed by a temperature sensor located in front of the fan. The fans start (minimum speed) when the temperature in the enclosure increases above +30 °C. If the inside temperature continues to increase, the fan speed will increase. As temperature decreases, fan speed also decreases. If a fan stops due to a failure, an alarm signal is sent to the power system's controller. Figure 3.2 in the below shows the appearance of the PBC 05 HC solar hybrid DC power system.

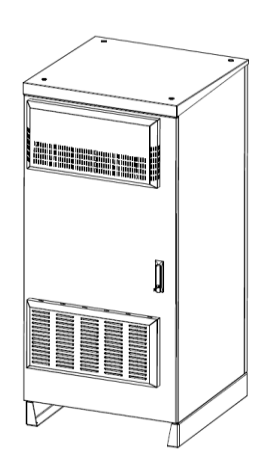


Figure 3.2: PBC 05 HC solar hybrid DC power system

Table 3.1 shows the mechanical characteristics of the PBC 05 HC solar hybrid DC power system.

Table 3.1: PBC 05 HC solar hybrid's mechanical characteristics

Width	Height	Depth
708 mm	1769 mm	789 mm

Table 3.2: PBC 05 HC solar hybrid's environmental characteristics

Description	Value
Operational temperature range	Maximum operational temperature: 50°C. Minimum temperature: According to the recommended minimum ambient temperature for the specific battery or 19" equipment to be installed.
Temperature range, transportation and storage	-40 to 70°C
Relative humidity	Normal operation: 15 to 100%
	Transportation: 5 to 100%

Table 3.3 shows the AC input characteristics of the PBC 05 HC solar hybrid DC power system.

Table 3.3: PBC 05 HC solar hybrid's AC input characteristics

Parameter	Value				
	Nominal: 200–250V AC				
Input Voltage	Range: 85–300V AC				
	1-, 2-, and 3-phase connection				
Line Frequency	45–65Hz				
Rectifier Efficiency	High-efficiency: 96%				
Rectifier Efficiency	230 V AC for 20%–90% load				
	20kA (L-N)				
AC Suma Protection	40kA (N-PE, nominal surge current,				
AC Surge Protection	8/20µs)				
	SPD class C (IEC/VDE)				

Table 3.4 shows the DC input characteristics for the solar MPPTs that are used in the PBC 05 HC solar hybrid DC power system.

Table 3.4: PBC 05 HC solar hybrid's DC input characteristics

Parameter	Value		
	Nominal: 140–400V DC		
Input Voltage	Range: 120–420V DC		
Line Frequency	45–65Hz		
Rectifier Efficiency	High-efficiency: 96%		

Table 3.5 shows the DC output characteristics of the PBC 05 HC solar hybrid DC power system.

Table 3.5: PBC 05 HC solar hybrid's DC output characteristics

Description	Value
Nominal Output Voltage	-48V DC (-15% / +20%)
Output Voltage Range	-42 o -58V DC.
	Rectifier module capacity: 2kW.
	Maximum number of rectifier modules: 9
	Total maximum rectifier capacity: 18KW.
Output Power	Solar MPPT module capacity: 2kW.
	Maximum number of solar MPPT modules: 9
	Total maximum solar capacity: 18KW.
	Total Maximum system capacity: 36KW.
	Main load distribution:12×13 mm wide CB
DC Distribution	positions
	Priority load distribution: 9×13 mm wide CB
	positions
CB Ratings (A)	150,125, 100, 80, 63, 50, 32, 25, 20, 16, 10, 6, 2 A
DC Surge Protection	The internal DC bus is surge protected with
	maximum surge current (8/20μs) is 15kA.
Battery Interface	2 x Circuit breakers each of 300A rating.

3.3 Solar Panels

Ericsson has considered mono-crystalline solar panels to fully comply with the requirements of the customer. The offered solar panels are manufactured by "Trina Solar "which is one of the biggest global and good manufactures for the solar panels. Table 3.6 shows the electrical characteristics of the offered solar panels.

Table 3.6: Solar panel's electrical characteristics

Parameter @ STC	Value
Peak Power (Wp)	270W
Power Output Tolerance-PMAX (%)	3%
Maximum Power Voltage	30.8V
Maximum Power Current	8.77A
Module Efficiency	16.5%
Open Circuit Voltage	38.6V
Short Circuit Current	9.23A

All the above-mentioned values are based on STC "Standard Test conditions "where Irradiance is 1000W/m², cell temperature is 25°C, air mass is 1.5 according to EN 60904-3. Table 3.7 shows the mechanical characteristics of the offered solar panels.

Table 3.7: Solar panel's mechanical characteristics

Parameter	Value			
Solar Cells	Mono-Crystalline			
Number of Cells per Panel	60Cells			
Solar Panel's Dimensions (H x W x D)	1650 mm x 992 mm x 35 mm			
Weight	18.6 KG			
Glass	High Transparency Solar Glass 3.2mm Black Anodized Aluminum Alloy			
Frame				

Table 3.8: Solar panel's different temperature ratings and coefficients

Parameter	Value
Nominal Operating Cell Temperature	44°C
Operating Cell Temperature Range	-40 to 85°C
Temperature Coefficient of PMAX	- 0.41%
Temperature Coefficient of VOC	- 0.32%
Temperature Coefficient of ISC	0.053%

Figure 3.3 shows the mono crystalline solar panels.



Figure 3.3: Mono-crystalline solar panel

3.4 Panel Support Structure

The function of the support structure is to hold the PV panels in place and enables the panels to be tilted in a desired angle towards the sun such that the optimum solar power is obtained. The support structure is built up by modules allowing the structure to de designed for a desired number of PV-panels. There are 4 different types of solar structure which are offered as in the below,

- A low level solar support structure which can support up to 8 solar panels.
- A low level solar support structure which can support up to 16 solar panels.
- A high level solar support structure which can support up to 8 solar panels.
- A high level solar support structure which can support up to 16 solar panels.

The type of the solar structure will be selected based on the site's configuration in a way where the surface area required by all solar structures can be minimized. The new PV-Max-S has a concrete foundation. The foundation of ground-mounted solar plants on concrete foundations is an efficient way of installing solar plants on sub soils that do not allow pile-

driving or when pile-driving would not be economically efficient. This also includes areas with chemically aggressive sub soils, as a foundation using driven piles made of steel is not easy or even impossible on such soils. PV-Max-S is also an option for small solar plants, because special soil surveys or test pile-driving would be too expensive and out of all proportion to the overall investment. Figure 3.4 shows an overview of the solar structure.



Figure 3.4: Solar structure's overview

3.5 Exide OPzS batteries

The Classic OPzS solar range from Exide has been well proven for decades in medium and large power requirements. Due to their robustness, long design life and high operational safety. They are ideally suitable for use in solar and wind applications, telecommunications, power distribution companies, railways and many other safety equipment power supplies. The wide range of available capacities and sizes provides a solution for every power need, even in harsh environments. The classic OPzS solar batteries have special alloy and large electrolyte reserve which can grant a very long topping up intervals which can be up to 3 years.

The main specifications of the solar OPzS batteries are:

- Nominal capacity range (C120 at 25 °C): 70 4600 AH.
- Very thick tubular positive plates for the most demanding applications.
- Up to 2800 cycles at 60 % depth of discharge (C10) with IU charging profile at 20 °C.
- Designed in accordance with IEC 61427 and IEC 60896-11.
- Screw connectors for a better contact and reliability.

- Available in two different versions dry-charged version with separate electrolyte or wet charged with filled in acid.
- High quality transparent containers for easy maintenance

Figure 3.5 shows the appearance of the OPzS solar batteries.



Figure 3.5: Exide's OPzS solar batteries

3.6 OPzS Battery Boxes

The OPzS solar batteries will be housed in outdoor boxes, the material of the boxes is a thermoplastic compound died in the mass, designed for outdoor use. It is also resistant to rapid temperature changes, shocks, UV, corrosion, chemical agents and pollution. The offered boxes has the following characteristics

- Protection degree: IP 43 as per IEC 60529.
- Shock resistance: IK 10 as per IEC 62262.
- Dielectric rigidity: 6 kV as per IEC 60950, transversal resistance of our material.
- Fire resistance: UL 94 V0.
- Acid resistance: no reaction while exposed to acids where in some cases the acid might escape from the batteries and affect some plastic materials (polyester) that turn grey or black. Thanks to their resistance to chemical aggressions, the boxes are made from thermoplastic

compound that do not have the same limitation and keep their aspect for years.

- Corrosion: corrosion free (thermoplastics)
- Thermal insulation: $K = 0.3 \text{ W} / ^{\circ} \text{ C} / \text{ m}^2$.

All the battery boxes are equipped with a 48V DC fan to grant sufficient ventilation for batteries. Also the battery boxes have cable glands where the battery cables can pass through to be connected directly to the battery terminals. All the battery boxes are equipped with a front door which can be used to check the acid level of the batteries. The battery boxes are delivered as kits and they have to be assembled on sites based on the supplied installation instructions. The battery boxes which will be used for housing the 1650 AH OpzS solar batteries can accommodate two battery strings in one box, However the boxes which will be used for the 3100 AH batteries can accommodate one battery string only due to the big dimensions of this battery capacity. The dimensions of the battery boxes which are considered for different battery capacities are:

• For the 1650 AH batteries,

(W x D x H): 2025 mm x 1890 mm x 1333 mm

• For the 3100 AH batteries,

(W x D x H): 2025 mm x 1485 mm x 1453 mm

All types of battery boxes are equipped with 48V DC fan, 165m3/h in order to secure the required ventilation for the batteries. Figure 3.6 in the below shows an overview for one of the offered battery boxes,



Figure 3.6: Battery box's overview

3.7 Diesel Generator

The Generator set is a fully integrated power generation system, providing optimum performance, reliability, and versatility for stationary prime power applications with primary feature strong motor starting capability and fast recovery from transient load changes. The torque-matched system includes a heavy-duty 4-cycle diesel engine, an AC alternator with high motor-starting KVA capacity, and a voltage regulator with three phase sensing for precise regulation under steady-state or transient loads. The Gen-Set accepts 100% of the nameplate standby rating in one step, in Compliance with NFPA110 requirements. Four different ratings are considered such that all the requirements of different applications like hybrid, solar hybrid and grid with backup DG are fulfilled. Tables 3.9 and 3.10 showing details related to the engine and alternator of the 30kVA DG respectively.

Table 3.9: F4L2011's engine details

Brand	Deutz, Germany
Model	F4L2011
Cylinders	4
Displacement	3.11 L
Induction system	Naturally Aspirated
Bore / Stroke	94 mm / 112 mm
Cooling system	Air cooled
Engine type	In-line, 4 cycle
Prime power	30 KVA
Standby power	31.5 KVA
Speed	1500 RPM
Governor	Mechanical

Starting system	12 V batteries
Comp. ratio	19:1
Oil capacity	5.5 L
Engine's weight	293 KG

♣ Alternator

Table 3.10: PI144G's technical details

Brand	SATMFORD
Model	PI144G
Insulation Class	Н
Phases	3 phases + Neutral
Connection	Series
Control system	Self-excited and
	brushless
Winding Pitch	2/3
Rated power factor	0.8
IP degree	23
AVR model	AS480
Regulation	1%
Weight	159 KG

3.8 The Site Design and Consideration

All the design dimensioning and calculations which are applied for the site under study are shown in this section.

♣ By using the considered coordinates where the latitude is 6.927 and the longitude is 37.83 into NASA solar meteorology web tool, the monthly average solar insolation is stated in table 3.11.

Table 3.11: Monthly average solar insolation values

Month	Jan	Feb	Mar	Apr	May	June	July	Aug	Sep	Oct	Nov	Dec
Solar insolation	5.96	6.33	6.3	5.91	5.71	5.19	4.68	4.97	5.55	5.77	6.07	5.97
kWh/m2/day												

- ♣ Total maximum power consumption of the radio, Transmission equipment, Climate system of the power cabinet and the climate system of the battery boxes to be used = 2,253 Watts
- Minimum required battery capacity to achieve 3 days' autonomy (Customer requirement) = (Total power consumption x required autonomy in hours) / (nominal voltage x Depth of Discharge) = (2253 x 72) / (48 x 0.8) = 4224.3 AH, as per table 3.12 in the below, the most adequate battery to be used from the offered battery capacity will be OPzS solar 3100 as its capacity at C72 is 2910 AH, So two battery strings each of OPzS solar 3100 will be used in order to fulfill the required 3 days autonomy.

Table 3.12: Different discharging rates of OPzS solar batteries

Туре	С ₆ 1.75 Vpc	C ₁₀ 1.80 Vpc	C ₁₂ 1.80 Vpc	C ₂₄ 1.80 Vpc	C ₄₈ 1.80 Vpc	C ₇₂ 1.80 Vpc	C ₁₀₀ 1.85 Vpc	C ₁₂₀ 1.85 Vpc	C ₂₄₀ 1.85 Vpc
OPzS Solar 190	122	132	134	145	165	175	185	190	200
OPzS Solar 245	159	173	176	190	215	230	240	245	260
OPzS Solar 305	203	220	224	240	270	285	300	305	320
OPzS Solar 380	250	273	277	300	330	350	370	380	400
OPzS Solar 450	296	325	330	355	395	420	440	450	470
OPzS Solar 550	353	391	398	430	480	515	540	550	580
OPzS Solar 660	422	469	477	515	575	615	645	660	695
OPzS Solar 765	492	546	555	600	670	710	750	765	805
OPzS Solar 985	606	700	710	770	860	920	970	985	1035
OPzS Solar 1080	669	773	784	845	940	1000	1055	1080	1100
OPzS Solar 1320	820	937	950	1030	1150	1230	1295	1320	1385
OPzS Solar 1410	888	1009	1024	1105	1225	1305	1380	1410	1440
OPzS Solar 1650	1024	1174	1190	1290	1440	1540	1620	1650	1730
OPzS Solar 1990	1218	1411	1430	1550	1730	1850	1950	1990	2090
OPzS Solar 2350	1573	1751	1770	1910	2090	2200	2300	2350	2470
OPzS Solar 2500	1667	1854	1875	2015	2215	2335	2445	2500	2600
OPzS Solar 3100	2080	2318	2343	2520	2755	2910	3040	3100	3250
OPzS Solar 3350	2268	2524	2550	2740	2985	3135	3280	3350	3520
OPzS Solar 3850	2592	2884	2915	3135	3430	3615	3765	3850	4040
OPzS Solar 4100	2775	3090	3125	3355	3650	3840	4000	4100	4300
OPzS Solar 4600	3099	3451	3490	3765	4100	4300	4500	4600	4850
OPzS Solar 280	203	206	229	250	296	304	287	294	338
OPzS Solar 350	245	257	284	311	374	383	355	364	424
OPzS Solar 420	284	309	322	354	420	432	408	417	482
OPzS Solar 70	55.0	51.5	63.7	69.4	78.4	79.8	81.0	82.7	92.9
OPzS Solar 140	95.4	103	108	118	141	145	136	139	162
OPzS Solar 210	131	154	162	177	206	217	203	210	234

- ♣ As per the solar insolation values stated in table 3.11 in the above the less insolation per year 4.68 KWh/m2/day and the Peak Power is 270 W per module and by considering 30% as power losses. The max power per PV module = (270 x 4.68 x 0.7)/1000=0.88 KWh/day.
- ♣ The total energy consumption value per day = 2253x24/1000 = 54.07KWh/day, the number of required solar panels will be =54.07/0.88=61.4, After Roundup 64 panels.
- ♣ Since the output of 8 solar panels can be connected to 1 MPPT module, then the number of required solar MPPTs will be 8 modules.
- ♣ Considering the number of the required solar panels which are 64, Then two high level support structure which can support up to 16 solar panels and two low support structure which can support up to 16 solar are required.

The choice between the high and the low support structure is done in a way to grant that all the cabinets like RBS cabinet, Power cabinet and battery boxes will be installed under the solar support structure.

Figure 3.7 shows a plan view for the distribution of the solar panels and the required clearance between the solar structures with each other's and the solar structures with the site's fence. The clearance between the site's fence and the solar structure is based on a fence of 2-meter-high, If the site's fence will be more than 2 meters then the clearance value must be changed in order to avoid any unexpected shading.

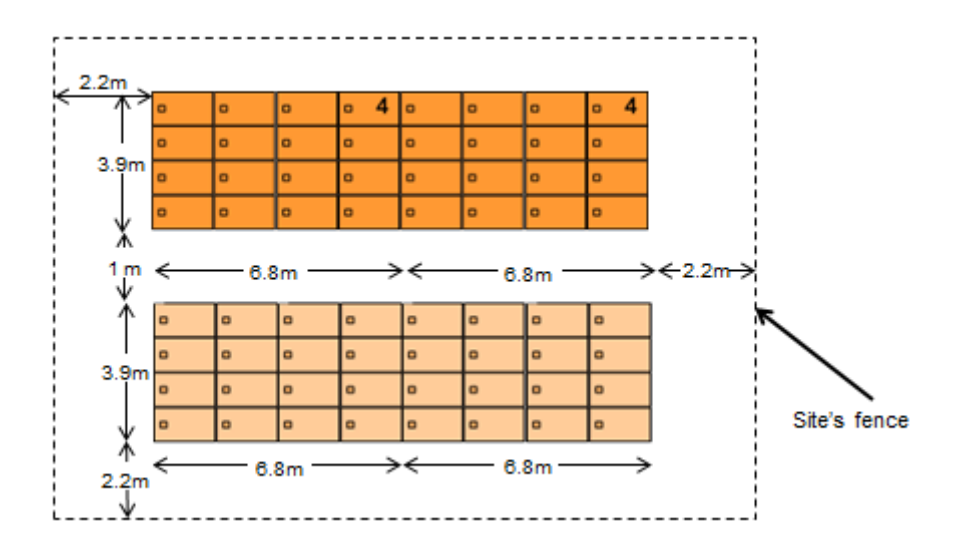


Figure 3.7: Plan view for the solar panels configuration

- ♣ Rectifier Module Number= (Load Current+ max Battery Charging Current)/ Single Rectifier Module Amperage Capacity Number of Rectifier modules = ((2253/48) +300)/40= 8.6 After Roundup = 9
- ♣ Total input power required by the rectifier modules which will be feeding loads and recharging the batteries = (Number of rectifier modules required to feed the loads and recharge the batteries x capacity per module) / (Module conversion efficiency x Module power factor) = (9 x2000) / (0.96 x 0.99) = 18939.4VA
- ♣ Minimum required DG capacity which shall be considered = Total required input power / (Maximum allowed loading percentage x (1 −

De-rating factor)) = 18939.4/(0.8*0.86) = 27528.2VA. As per the available DG capacities, the most adequate DG capacity to be offered will be the 30 KVA.

3.9 Summary

The summary of the proposed solution for site under study:

- ♣ PBC 05 HC solar hybrid DC power cabinet with 8 solar MPPTs and 7 rectifier modules, the cabinet will be equipped with 6 x 25 A circuit breakers to feed the 6 remote radio units, 1 x 150 A circuit breaker to feed the RBS 6301 cabinet, 2 x 20 A circuit breaker to feed the DC fan of the battery box and 2 x 6 A circuit breaker to feed the Ericsson site controller that will be installed inside the free space of the PBC 05 solar cabinet.
- ♣ 64 solar panels each of 270 Wp in addition to, two high level support structures each will be mounting 16 solar panels and another two low level support structures each will be mounting 16 solar panels, each 8 solar panels will be forming one string which will be connected to one MPPT modules through a SPD box.
- ♣ Two battery boxes, each will be housing one battery string of 3100 AH C120. Each battery string will be connected to 150 A battery circuit breaker in the PBC 05 HC solar hybrid DC power cabinet.
- 4 30 KVA DG with a built in ATS of rating 50 A.
- ♣ A separate fuel tank of 5000 L capacity.

CHAPTER FOUR

SYSTEM MODELING AND SIMULATION RESULTS

4.1 Introduction

This chapter will present the modeling and simulation results for the solardiesel hybrid power system with back up batteries applied for telecom load. The power applications and system design, modelling and simulation are essential to optimize control and enhance system operations.

The following subsections present the implementation of the PV/diesel and rectifier /lead acid battery hybrid system model. Modelling and simulation are implemented using MATLAB/ SIMULINK and SIMPOWERSYSTEM software packages. The block diagram of the developed hybrid power system is shown in Figure 4.1.

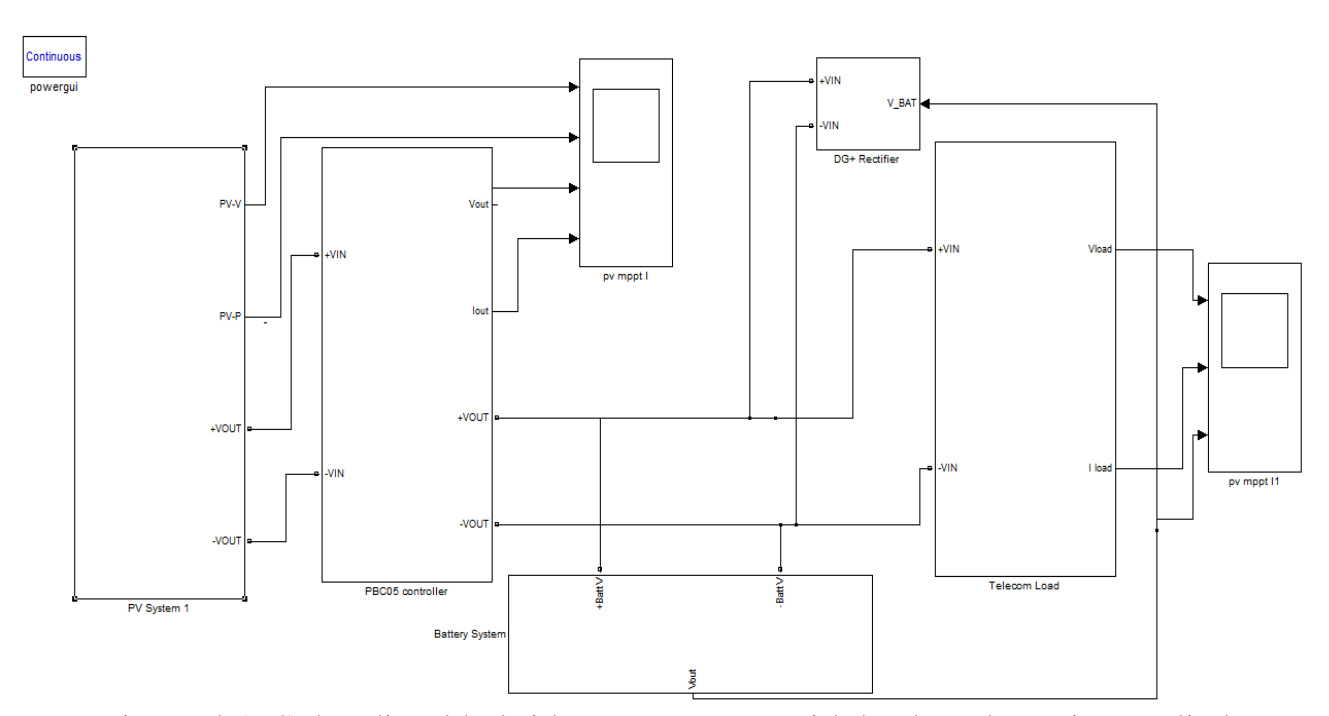


Figure 4.1: Solar-diesel hybrid power system with back up batteries applied for telecom load Simulink model

4.2 Simulink Model Construction of PV System

The PV array block implements an array of photovoltaic modules. The array is built of strings of modules connected in parallel, each string consisting of modules connected in series. The PV array block is a five-

parameter model using a current source IL (light-generated current), diode (*I*₀ and nI parameters), series resistance Rs, and shunt resistance Rsh to represent the irradiance- and temperature-dependent I-V characteristics of the modules.

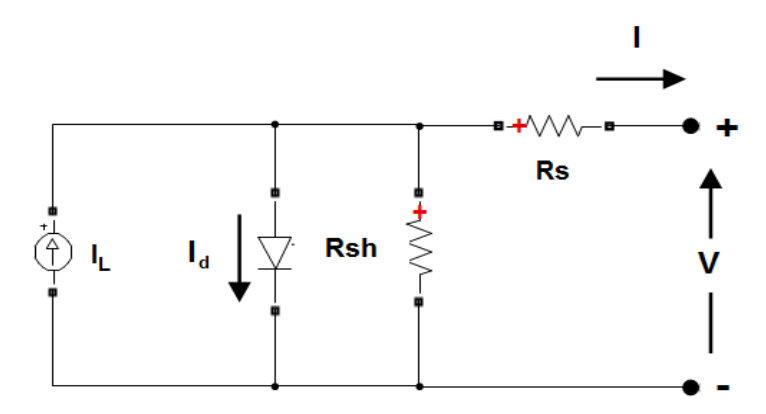


Figure 4.2: Equivalent circuit for the Solar Cell

Where:

Irradiances (W/ m^2): This parameter is available only if Display I-V and P-V characteristics of specified irradiances or array @ 25 deg. C and specified irradiances. is a vector of irradiances in W/ m^2 the design we consider it 1000 W/ m^2 .

Light-generated current IL (A): Current for one module under STC, flowing out of the controllable current source that models the light-generated current.

Diode saturation current I_{\circ} (A): Saturation current of the diode modeling the PV array for one module under STC. An optimization function determines this parameter to fit the module data and it is controlled by the vector of irradiances.

Shunt resistance Rsh (ohms): Shunt resistance of the model for one module under STC and the selected value is 550 ohm.

Series resistance Rs (ohms): Series resistance of the model for one module under STC and the selected value is 0.04 ohm.

Because of the PV array block is connected to a detailed power electronic converter where real switches are simulated, we need to specify a small

sample time to get accurate resolution in output curves. Figure 4.3 shows the PV system Simulink model.

4.3 Simulink Model Construction of Buck DC-DC Converter

To obtain a nonlinear model for power electronic circuits, one needs to apply Kirchhoff's circuit laws. To avoid the use of complex mathematics, the electrical and semiconductor devices must be represented as ideal components (zero ON voltages,

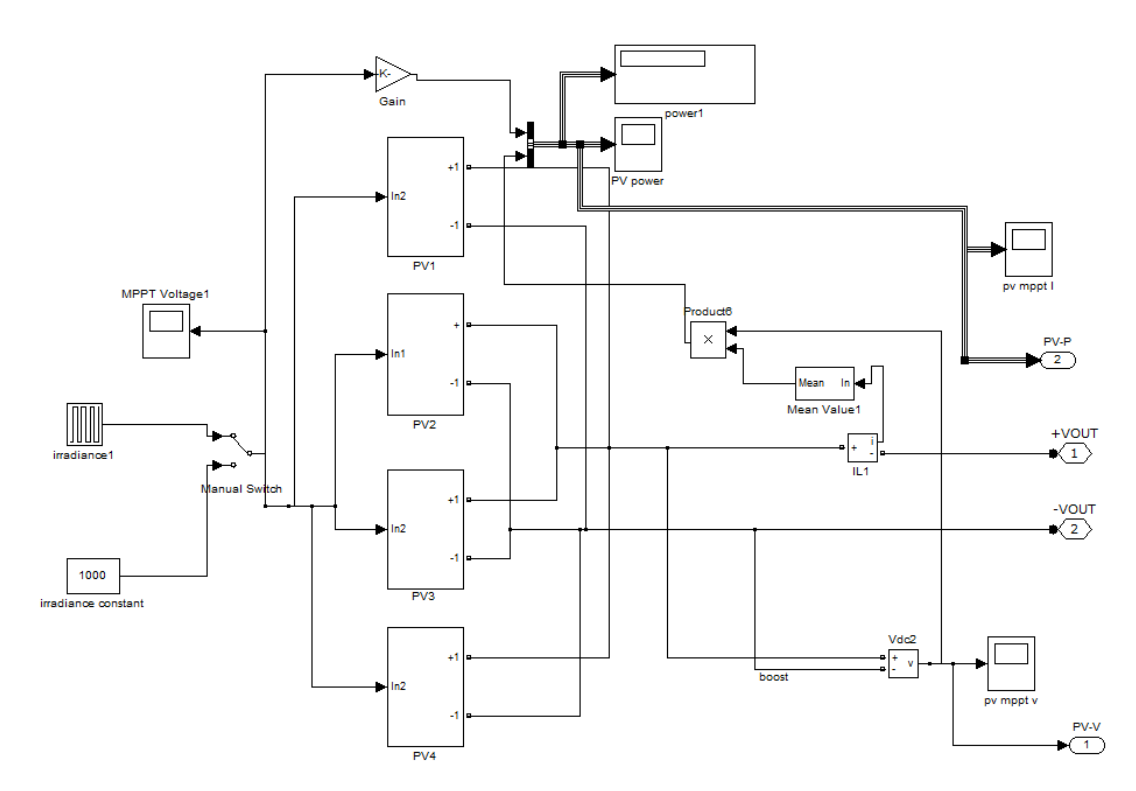


Figure 4.3: PV system Simulink model

zero OFF currents, zero switching times). Therefore, auxiliary binary variables can be used to determine the state of the switches. It must be ensured that the equations obtained by using Kirchhoff's laws should include all the permissible states due to power semiconductor devices being ON or OFF. Figure 4.4 shows the buck converter circuit diagram.

As shown in Figure 4.4, the buck converter consists of a DC supply or a rectified AC output, two switches i.e. D (diode) and S (can be semi-controlled or fully-controlled power electronics switches), two-pole low-pass filter (L and C) and a load. Let the duty ratio of switch S be:

$$D = \frac{T_{ON}}{T} \tag{4.1}$$

Where:

$$T = T_{ON} + T_{OFF} \tag{4.2}$$

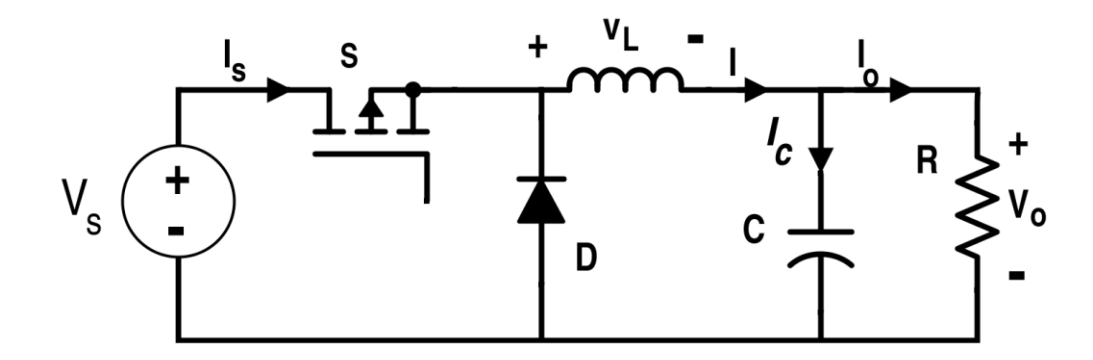


Figure 4.4: Buck converter circuit diagram

This circuit can be studied in two different modes. The first mode is when the switch S is on while the second mode is when the switch S is off. The circuit diagrams when the switch S is ON is given in Figure 4.5.

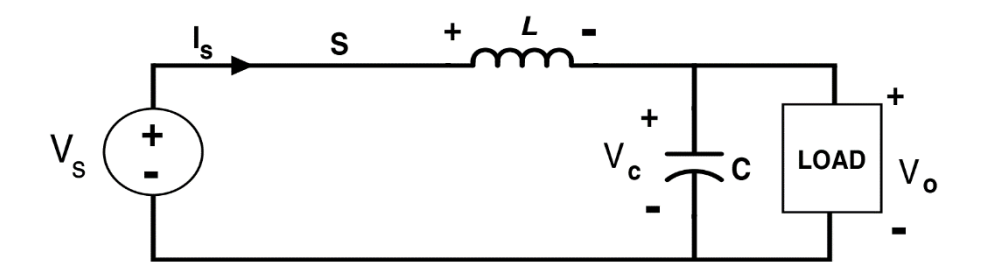


Figure 4.5: Buck converter circuit when switch S is On (Mode-I)

The Voltage across the inductor is defined by:

$$V_L = L \frac{dI}{dt} \tag{4.3}$$

Where:

$$I = I_C + I_{\circ} \tag{4.4}$$

The load current I_{\circ} can be calculated as:

$$I_{\circ} = \frac{V_{\circ}}{R} \tag{4.5}$$

When the switch S is on and applying the Kirchhoff's Voltage Law (KVL), we can get,

$$V_S = V_L + V_\circ = L \frac{dI}{dt} + V_c \tag{4.6}$$

Figure 4.6 shows the buck converter circuit when switch S is off.

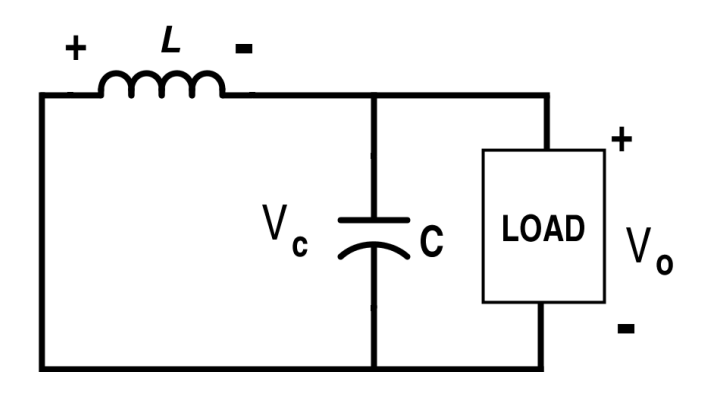


Figure 4.6: Buck converter circuit when switch S is Off (Mode-II)

When the switch S is off, the KVL in Fig 4.6 gives,

$$V_L + V_0 = 0 \tag{4.7}$$

$$\Rightarrow V_L = -V_{\circ} \quad \Rightarrow \quad V_{\circ} = -L \frac{dI}{dt} \tag{4.8}$$

As the output voltage is assumed constant by the small-ripple approximation,

$$\Rightarrow L \frac{dI}{dt} = \text{constant} \tag{4.9}$$

Waveforms of the voltage and current during the one-cycle period are shown in Fig 4.7

$$(I_{max} - I_{min})_{SWITCH-ON} = \frac{V_S - V_{\circ}}{L}DT$$
(4.10)

And

$$(I_{max} - I_{min})_{SWITCH-OFF} = -\frac{V_{\circ}}{L}(1 - DT)$$
(4.11)

$$\Rightarrow$$
 Average Inductor Current $=\frac{I_{max}-I_{min}}{2}=I$

From Figure 4.7 and from the steady-state perspective, magnitude of the inductor current increment during switch on is equal to the inductor current decrement during switch off; i.e.

$$|(I_{max} - I_{min})_{SWITCH-ON}| = |(I_{max} - I_{min})_{SWITCH-OFF}|$$

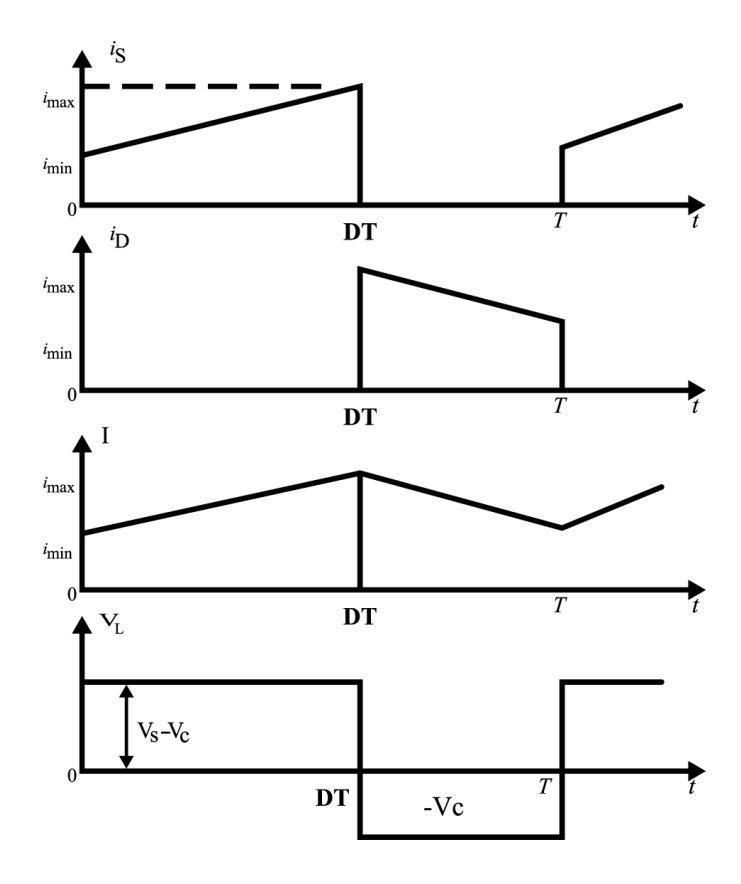


Figure 4.7: Supply current is, diode current id, inductor current i, and inductor voltage V_L waveforms respectively (buck converter)

$$\Rightarrow \frac{V_{\mathcal{S}} - V_{\circ}}{L} DT \mid = \mid -\frac{V_{\circ}}{L} (1 - DT) \mid \tag{4.12}$$

In the case of the buck converter, output voltage is directly dependent on the duty cycle and the input voltage.

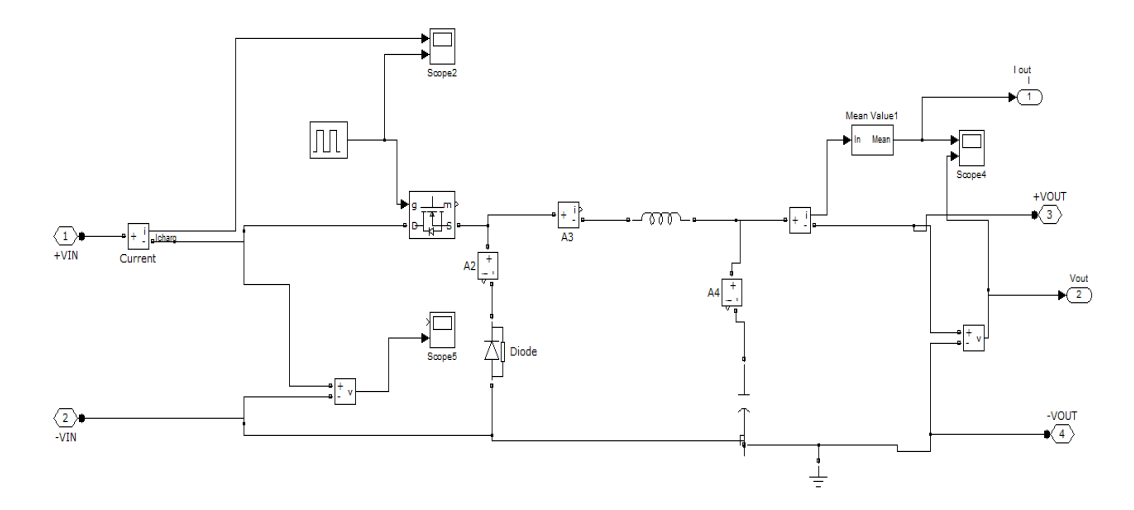


Figure 4.8: Buck converter Simulink model

4.4 Simulink Model for Battery System

The Battery block implements a generic dynamic model parameterized to represent most popular types of rechargeable batteries. The parameters of the equivalent circuit can be modified to represent a particular battery type, based on its discharge characteristics. A typical discharge curve is composed of three sections, as shown in figure 4.9.

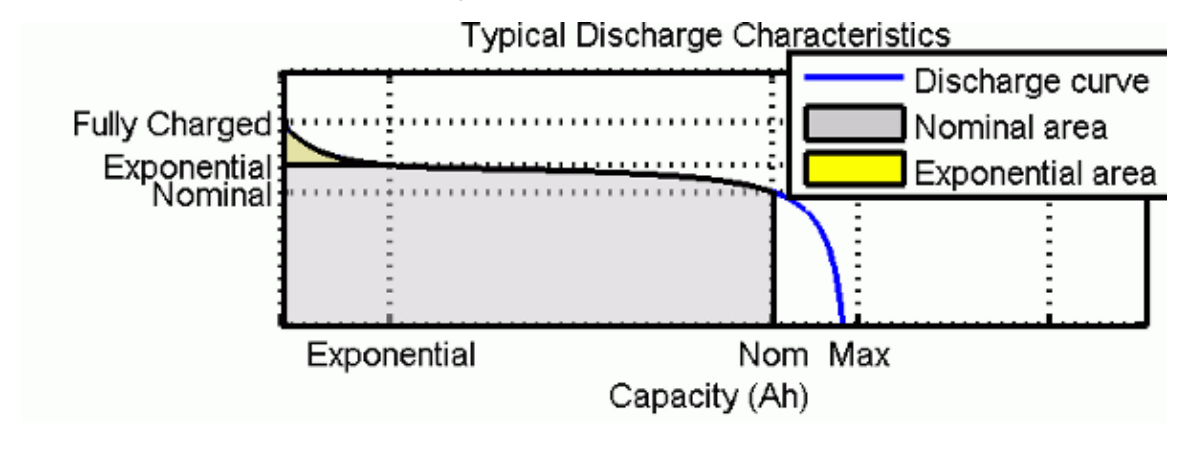


Figure 4.9: Battery discharge characteristics

The first section represents the exponential voltage drop when the battery is charged. Depending on the battery type, this area is more or less wide. The second section represents the charge that can be extracted from the battery until the voltage drops below the battery nominal voltage. Finally, the third section represents the total discharge of the battery, when the voltage drops rapidly. When the battery current is negative, the battery will recharge following a charge characteristic as shown in figure 4.10.

Note that the parameters of the model are deduced from discharge characteristics and assumed to be the same for charging. Figure 4.11 shows the battery system Simulink model.

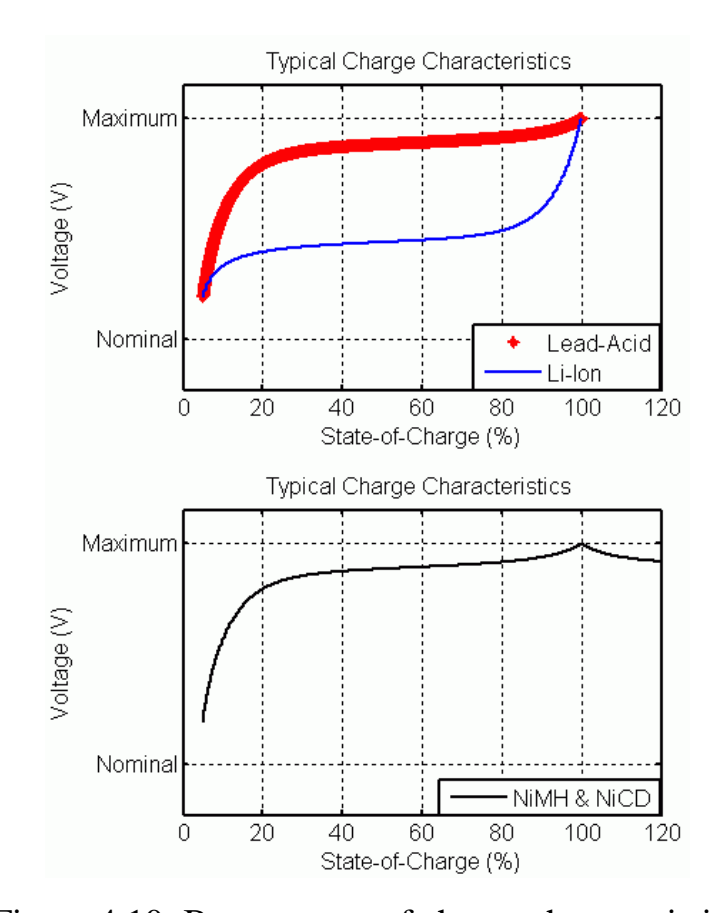


Figure 4.10: Battery state of charge characteristics

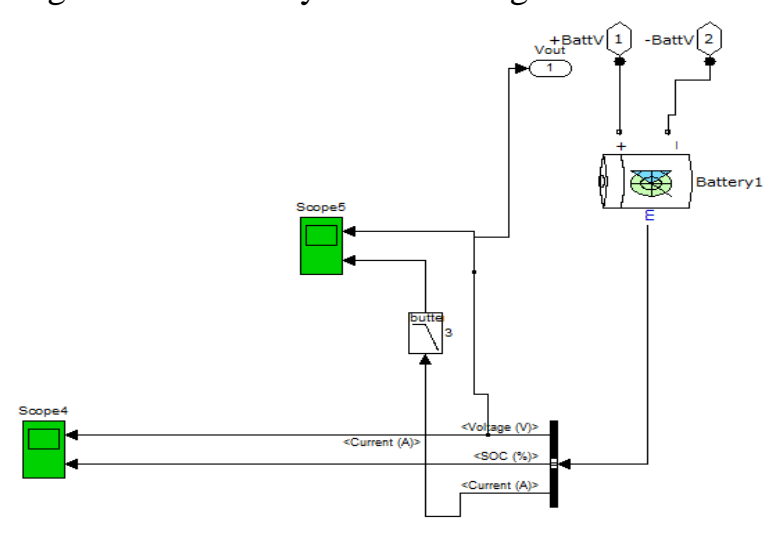


Figure 4.11: Battery system simulink model

.

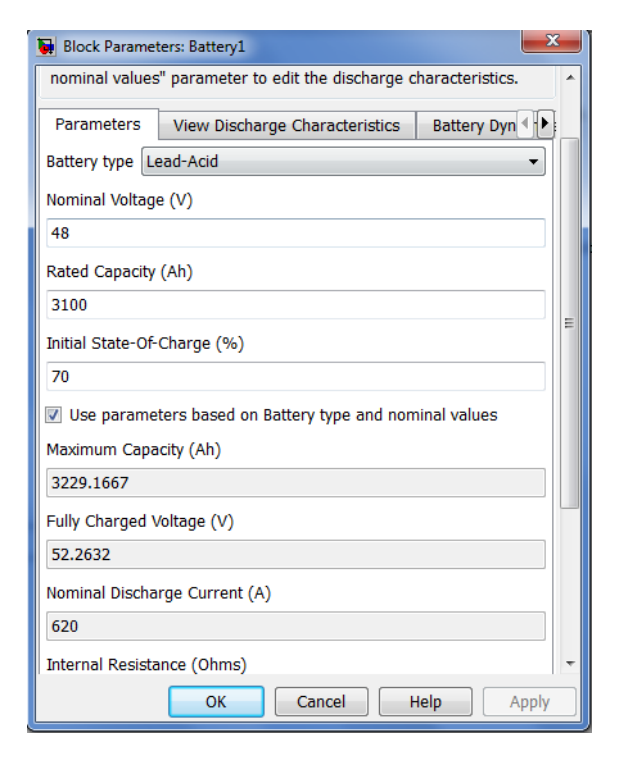


Figure 4.12: Battery system parameters values.

4.5 Simulink Model for DG, Rectifier, and telecom load system

The DG will work as backup when the battery voltage is less than the minimum operating voltage for the telecom load so the rectifier system will convert the AC power to DC. The DG and rectifiers are simulated using fixed DC source controlled by the battery voltage value as shown in Figure 4.13

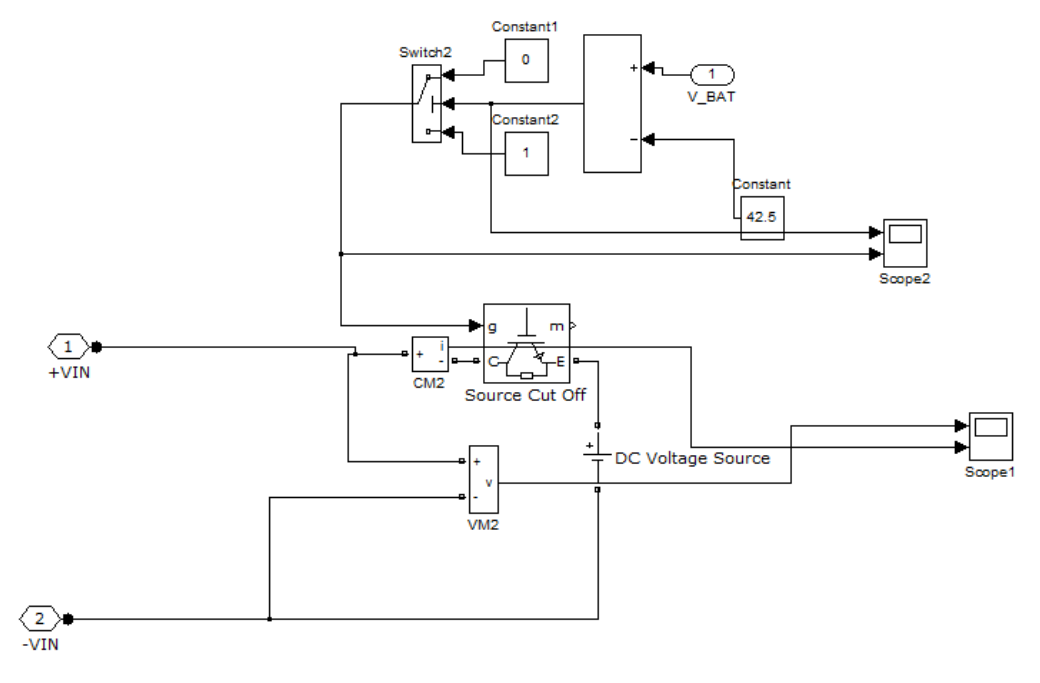


Figure 4.13: Simulink model for the DG and rectifier system

Figure 4.14 shows the flow chart of DG and rectifier control system.

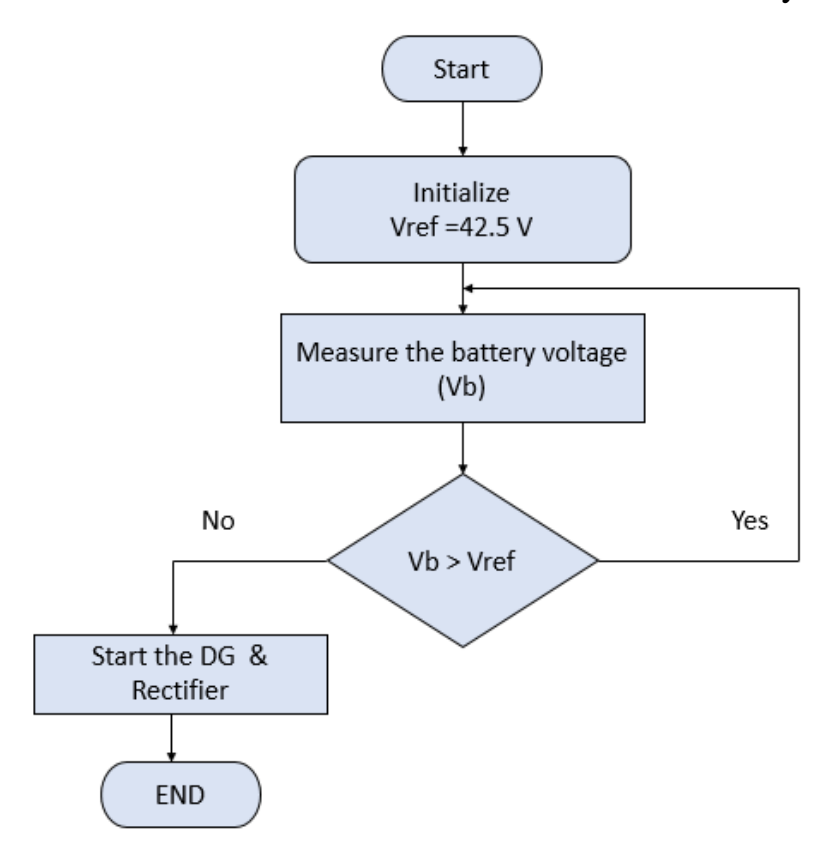


Figure 4.14: DG and rectifier control system flow chart

As the telecom load is working with DC it can be simulated as resistive load as shown in Figure 4.15.

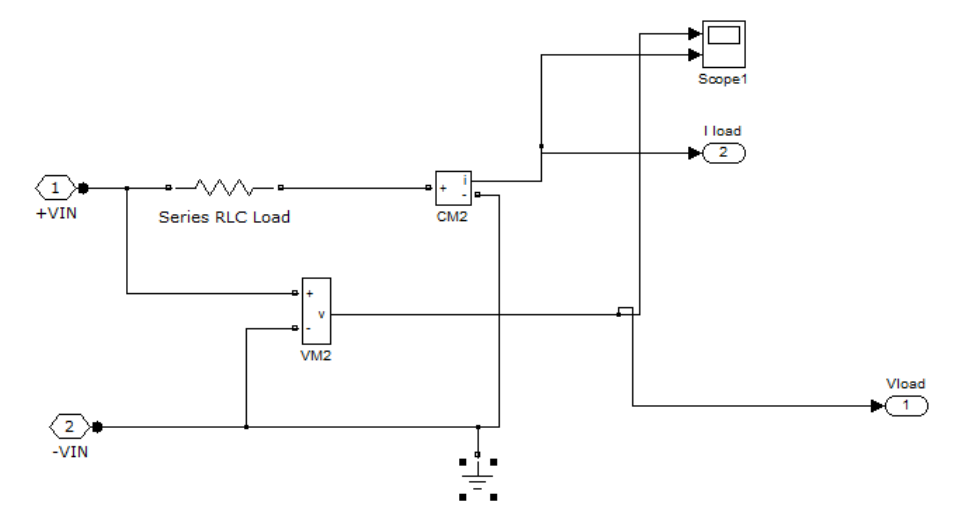


Figure 4.15: Simulink model for the telecom load.

4.6 Simulation Results

This section presents the simulation results compared with real data taken from the real telecommunication site. The simulation was set up as discussed in pervious sections where the system is working under the PV system, batteries and DG+ Rectifier is working as backup system. The real data was captured from the Ericsson monitoring system as shown in figure 4.16. The monitoring system is measuring the solar converter input voltage also is showing the battery voltage, current and SOC in addition to load voltage and current.



Figure 4.16: The hybrid sites Monitoring system GUI.

This monitoring system is receiving the actual data from the installed sensors in the sites which will be saved in the storage server. This server is showing all these data in the graphical user interface (GUI) as shown Figure 4.16. Below is comparison between the simulation and real site results.

4.6.1 PV system output voltage

Figures 4.17 and 4.18 shows the PV system output voltage from the real site simulation, respectively. From the real system, it can be seen that the output voltage is staring around 6:45AM as this is the time that the sun rises in area of this site and it continue till 18:00PM. The output voltage is changing during the day time between (200 - 300)V and due to many factors, the important ones are the PV cell Temperature and the shadow due to the clouds.



Figure 4.17: The monitoring system PV output voltage

From simulation, it considered that the sun rises at 0.06 sec which is equivalent to 6:00AM it considers fixed irradiance and temperature effects can be ignore. The sunset is around 0.18 which is equivalent to 18:00PM and it will be repeated on the next day at 6:00AM which will be after 30 hours from the beginning and it will continue like that.

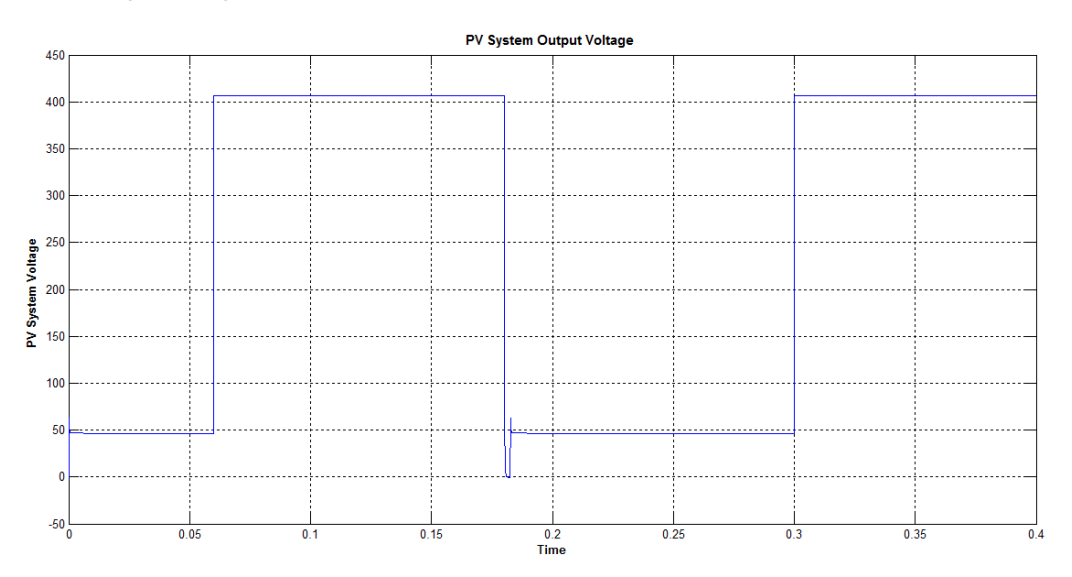


Figure 4.18: Simulation for PV system output voltage

4.6.2 PV system output current

In real site, there was no sense for the output current from the PV system. Figure 4.19 shows only the PV system simulation output current.

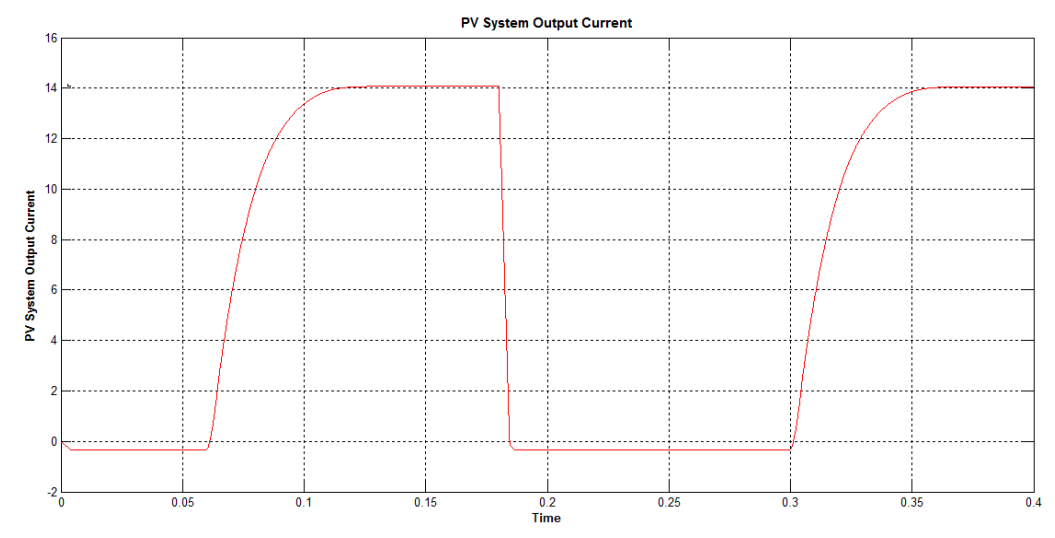


Figure 4.19: Simulation for PV system output current

From the simulation results it consider that the sun rises at 0.06 sec which is equivalent to 6:00 AM at that time the voltage is fixed but the current will start increasing exponentially till 14A the system will continue in 14A till the sunset and it will start in the next day following same concept.

4.6.3 DC-DC converter output voltage and current

The DC-DC converter is used as electronic MPPT to control the output power to the load. The converter is receiving the PV system output power and converts it to the required voltage and power. Figure 4.20 shows the simulation results for DC-DC converter output.

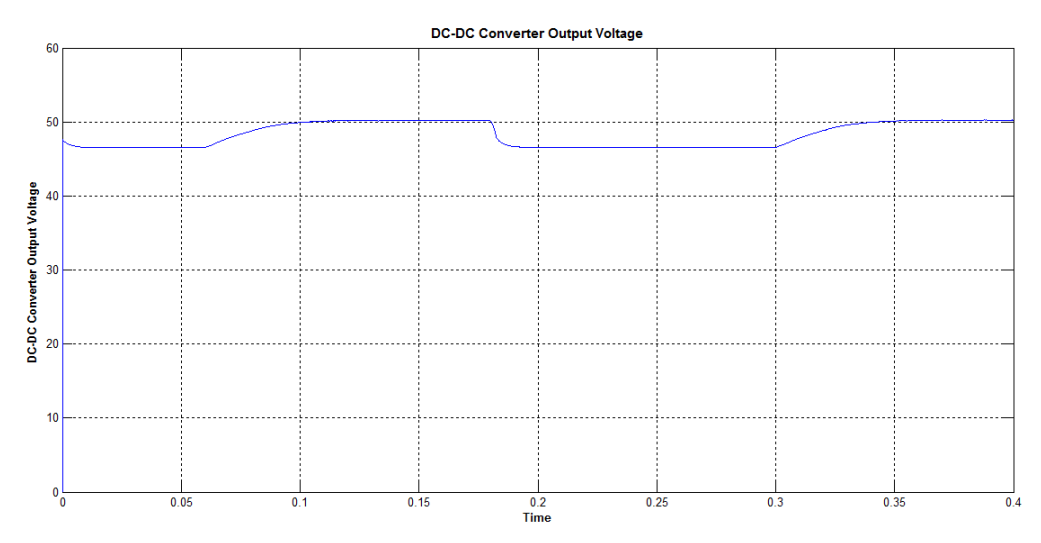


Figure 4.20: Simulation for DC-DC converter output voltage

The DC-DC converter output voltage is following the input voltage from PV system as the system voltage is equal to the battery voltage in the beginning

of the time from 0 to 0.06 in that time the voltage of the PV system will start increasing to 400V accordingly the DC-DC converter system output voltage will increase to 50V and will be stable till the sunset after that the output voltage is equal to the battery voltage. Figure 4.21 shows the simulation result for DC-DC converter output current.

The DC-DC converter output current start when there is power coming from the PV system and that will start after the sunrise at 0.06 which equivalent to 6:00AM at that time the current will start increasing exponentially till 105A.

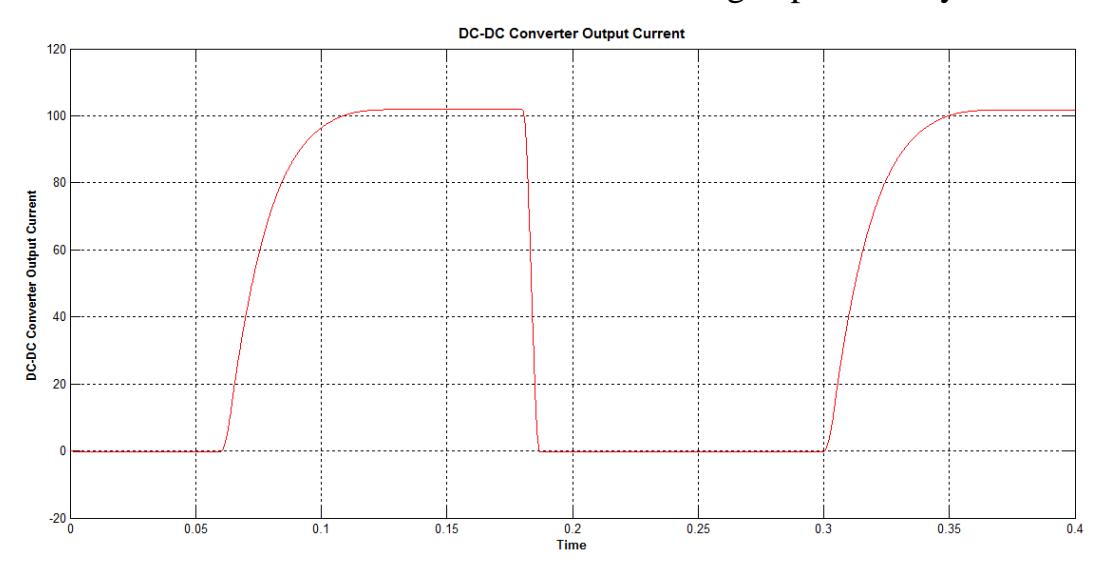


Figure 4.21: Simulation for DC-DC converter output current

The current will be stable in 105A for period after that it start decreasing at sunset time 0.18 sec. At this time there will not be any current following throw DC-DC converter.

4.6.4 The load output voltage and current

The telecom load rated voltage is 48V and the minimum operating voltage for all the equipment is 42.5V due to that the system voltage must not go below this value as showing in below plots for the voltage and current the voltage is 48V when the system is running with battery only and when the sunrise the output voltage will become the DC-DC converter output voltage. Figures 4.22 and 4.23 show the simulation results for load output voltage and current, respectively.

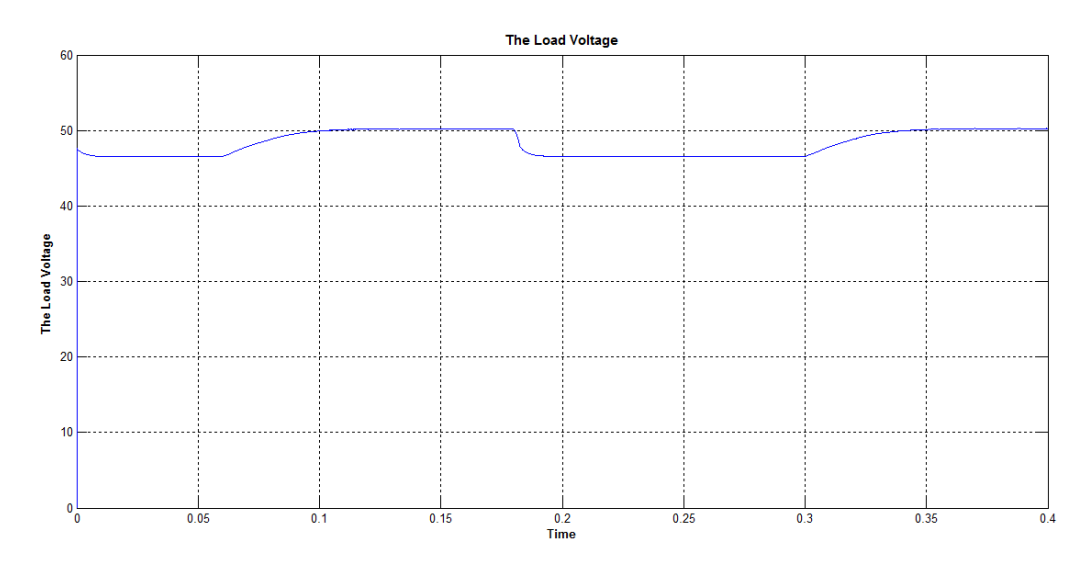


Figure 4.22: Simulation for the load output voltage

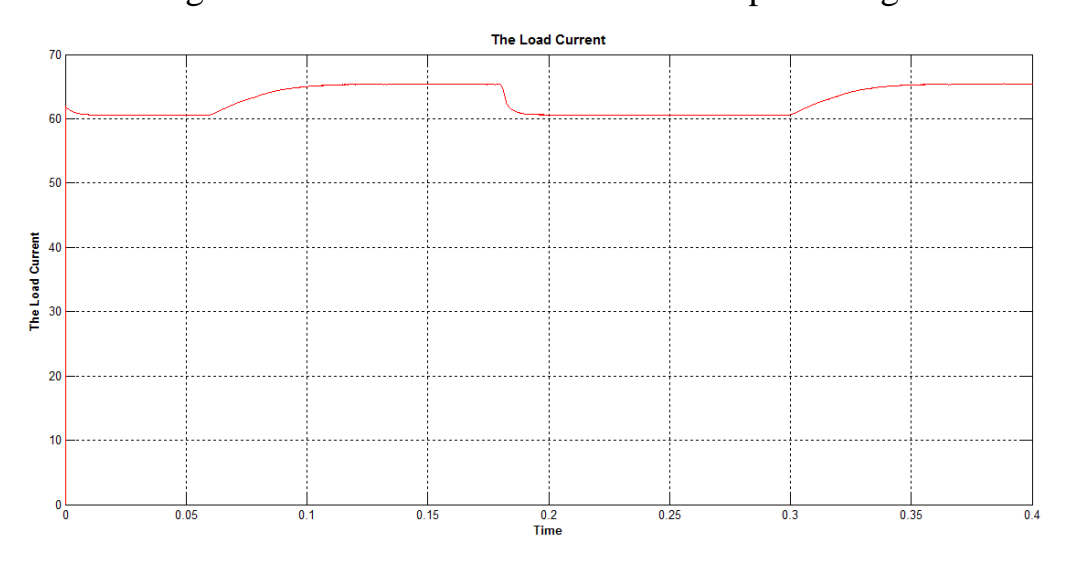


Figure 4.23: Simulation for the Load Output current

4.6.5 The battery voltage, current and SOC

The battery system plays very important role in the hybrid system as it is the main protection for the load during the change between the different operation modes. Figures 4.24 and 4.25show the battery voltage output from the real site and simulation, respectively. When the DC output voltage from the DC-DC converter start increasing above the rated voltage the battery will start charging and the voltage will be the same to the DC-DC converter output.



Figure 4.24: The monitoring system battery voltage

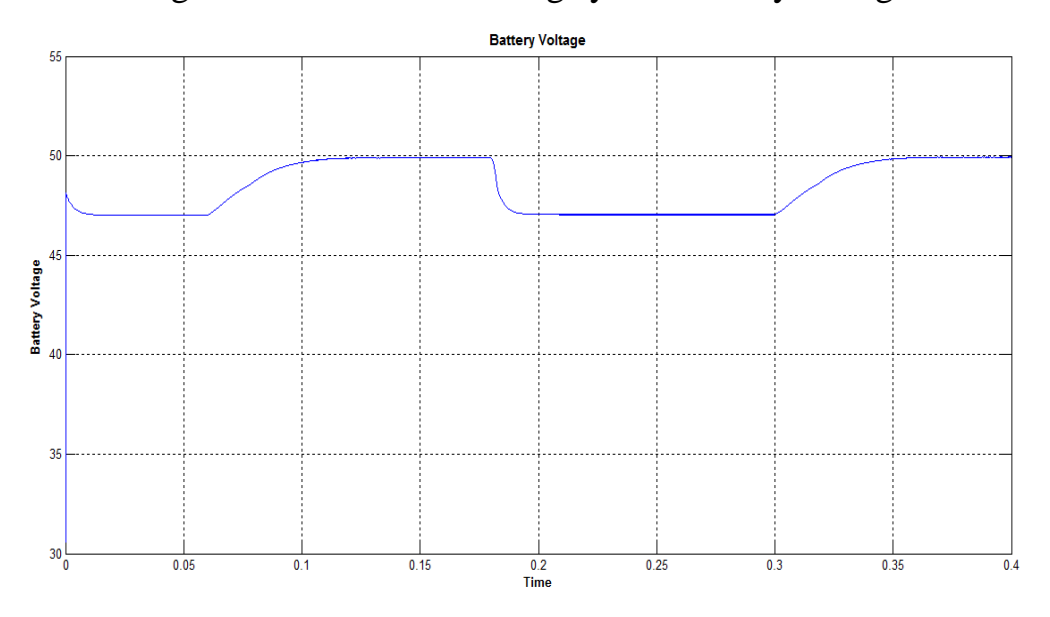


Figure 4.25: Simulation for the battery voltage

The rated voltage for the battery is 48V and the initial SOC was considered 70%, so the battery starts discharging since there was no sun at that time. When sunrise at 0.06 the voltage will start increasing as the DC-DC converter voltage is higher than the battery voltage. After the voltage is reaching the peak value around 50V it will be stable till the sunset around 0.18 so after that time the voltage will be the battery voltage. Figures 4.26 and 4.27 show the battery output current from the real site and simulation, respectively.



Figure 4.26: The monitoring system battery current

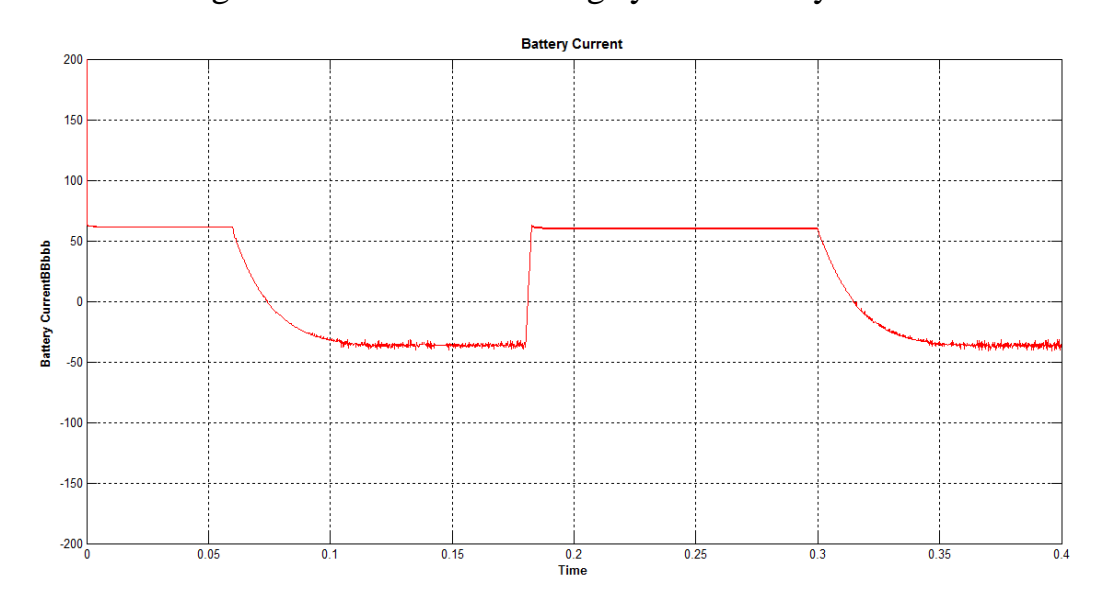


Figure 4.27: Simulation for the battery current

The battery current had two states, first when the battery is charging where the value will be in negative and the second when the battery is discharging and it will be the value in positive. As shown in Figure 4.27, the battery was discharging current around 60A as there is no sun yet till the sunrise time at 0.06 at this time the DC-DC converter voltage is higher that the battery voltage so the current will charge the battery so the current value will be in negative. The battery will be charging till the sunset 0.18 as at this time there is no power coming from the DC-DC converter. Figures 4.28 and 4.29 show the battery state of charge from the real site and simulation, respectively.

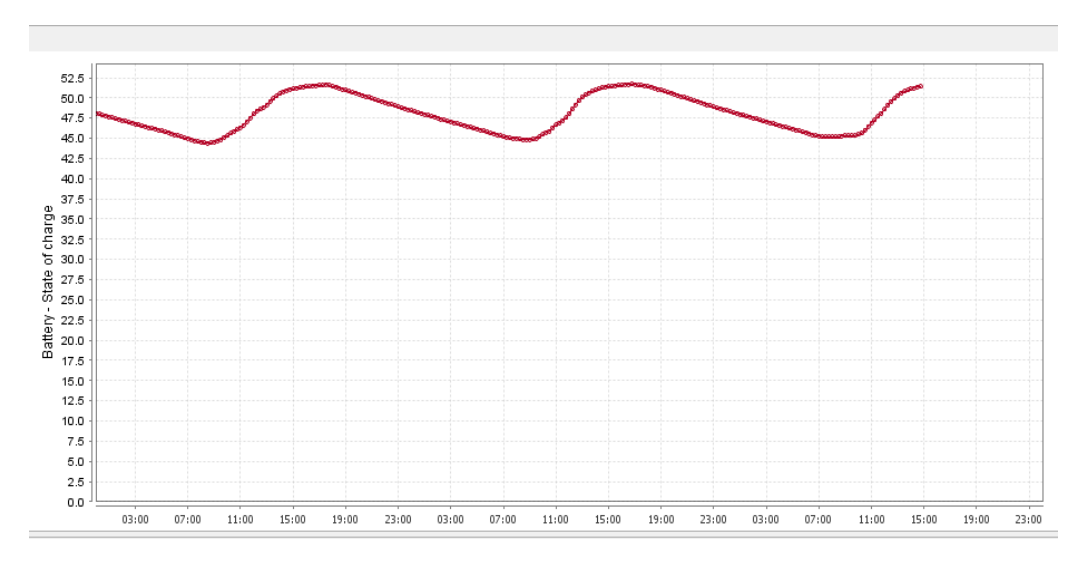


Figure 4.28: The monitoring system battery sate of charge

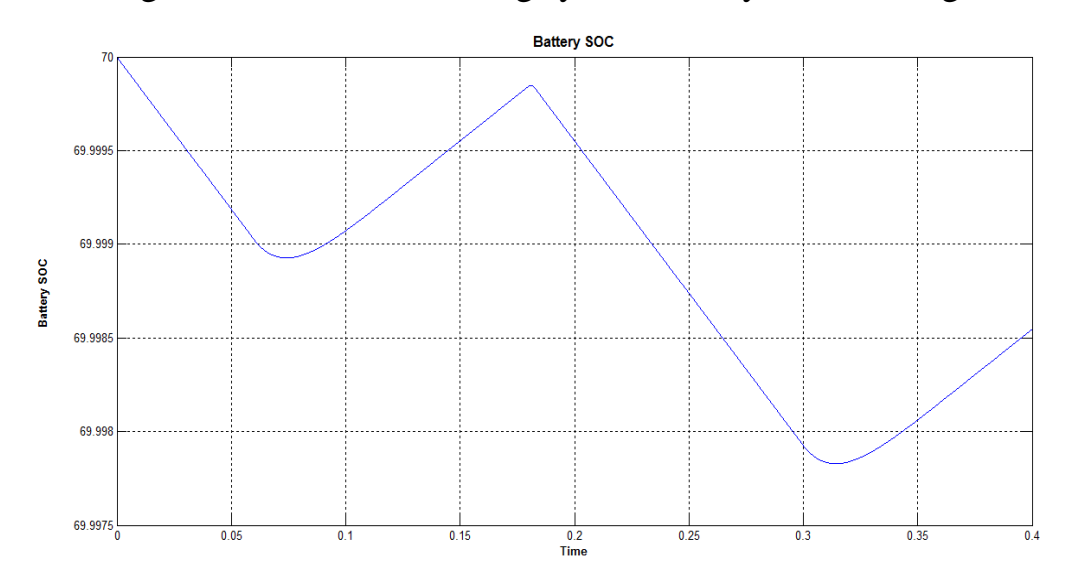


Figure 4.29: Simulation for the battery state of charge

The state of charge value will be changing with all battery operation status. The first value must be more than 70% so for that when there is new solar site they must charge the batteries from other source before they connect it to the solar system. In the simulation, we set the start SOC for the battery is 70% so the first period battery starts discharging till 69.998% till the sunrise time 0.06 at that time the battery starts charging so the SOC will start increasing till the sunset time and it will continue the same way.

CHAPTER FIVE

CONCLUSION AND RECOMMENDATIONS

5.1 Conclusion

The solar, batteries and diesel hybrid power system for telecom site was our target in this study in term of system design and performance. This site was implement by Ericsson and the real data was taken as inputs for the simulation.

The Simulation results and the real reading from the site was approximately the same because of the real sites have changeable working conditions not like the ideal condition which were considered for the simulation. The PV system was assessed by considering fixed sun irradiance and ignoring temperature effect and by capturing the output voltage and current to see the effect of changing Irradiance. From real site, the PV system output voltage was captured and the simulation Irradiance profile was adapted according to the real site performance. As the needed rated voltage for the telecom load and battery is 48V, the DC-DC converter was considered to give stable output voltage for telecommunication load and for charging batteries.

In design of the real site the sun absent was consider for three days as it will be cloudy during the raining seasons so the battery system capacity must be enough for load for three days without any charging. The battery system performance was capture from the real site in form of battery voltage, current and state of charge.

In the simulation, the battery was design with the same specification to have the same performance and for purpose of comparison. As backup system, DG connected to rectifier system was considered to take over if there was any issue with battery system with simple control logic following the busbar voltage. The load was considered as resistive load and the voltage and current were captured during the simulation period. The simulation time was very small to reduce the running time as the design system is very complicated and

contents a lot of inductors and capacitors which is putting huge delay to complete the simulation.

The benefit from this study that it's explaining how to design the hybrid system in detail and it show how we can evaluate the performance of this site in term of the stability and efficiency.

5.2 Recommendations

The solar, batteries and diesel hybrid power system is very effective for small scales application due to many factors like the cost and the performance so from this study we can recommend getting stable performance we can use higher battery capacities to be sure from the power availability for our loads. Also, we can ignore the DG and rectifier part for noncritical load to reduce the capital cost. Future studies are:

- Using fuel cells to replace the costly batteries in hybrid system.
- Using DC generators in place of the DG and rectifier to reduce the cost.
- Introduce new source like wind for the high areas.
- To apply the same system for agriculture applications.

REFERENCES

- [1] Lindsey Grant, "The End of Fossil Fuels", Negative Population Growth, PP 1-12, October 2004.
- [2] LaMar Alexander, "Simple Solar Homesteading Off The Grid", Lamar Alexander and SunPower publishing, Vol. 112, Pt. A, No.6, 2007.
- [3] J. Chadjivassiliadis," Solar Photovoltaic and Wind Power in Greece", IEE proceedings, Vol. 134, Pt. A, No. 5, May 1987.
- [4] Oscar Buneman, Torsten Neubert, and Ken Ichi Nishikawa, "Solar Wind-Magnetosphere Interaction as Simulated by a 3-D EM ", IEEE Transaaions on Plasma Science, Vol. 20, No. 6, December 1992.
- [5] Riad Chedid and Saifur Rahman, "Unit Sizing and Control of Hybrid Wind-Solar Power Systems": John Astron, IEEE Transactions on Energy Conversion, Vol. 12, No. 1, March 1997.
- [6] S. Arul Daniel and N. AmmasaiGounden, "A Novel Hybrid Isolated Generating
- System Based on PV Fed Inverter-Assisted Wind-Driven Induction Generators",: IEEE Transactions on Energy Conversion, Vol. 19, No. 2, June 2004.
- [7] Lingfeng Wang and Chanan, "Multicriteria Design of Hybrid Power Generation
- Systems Based on a Modified Particle Swarm Optimization Algorithm",: IEEE Transactions on Energy Conversion, Vol. 24, No. 1, March 2009.
- [8] Toshiro Hirose and Hirofumi Matsuo, "Standalone Hybrid Wind-Solar Power Generation System Applying Dump Power Control Without Dump Load", IEEE Transactions on Industrial Electronics, Vol. 59, No. 2, February 2012.
- [9] Chem V Nayar, "A Solar/Mains/Diesel Hybrid Uninterrupted Power System A Project Implemented in India", Centre for Renewable Energy Systems Technology Australia (CRESTA), 1997.

- [10] Xiangjun Li, Dong Hui and Xiaokang Lai, "Battery Energy Storage Station (BESS)-Based Smoothing Control of Photovoltaic (PV) and Wind Power Generation Fluctuations", IEEE Transactions on Sustainable Energy, Vol. 4, No. 2, April 2013.
- [11] C.V. Nayar, M. Ashari and W.W.L. Keerthipala, "A Grid-Interactive Photovoltaic uninterruptible power supply System using Battery Storage and a Backup Diesel Generator", IEEE Transactions on Energy Conversion 15 (2000) 348-353.
- [12] R. Ruther, "D.C. Martins and E. Bazzo. Hybrid Diesel/Photovoltaic Systems Without Storage for Isolated Mini-grids in Northern Brazil", Photovoltaic Specialists Conference, 2000.
- [13] R.L.G. E.L. Maxwell, "A Climatological Solar Radiation Model", in The 1998 American Solar Energy Society Annual Conference, T.C. R. Campbell-Howe, B. Wilkins-Crowder, Editor. 1998, American Solar Energy Society: Albuquerque, NW. pp. 505-510.
- [14] C.D. Barley and C.B. Winn, "Optimal Dispatch Strategy in Remote Hybrid Power Systems", Solar Energy 58 (1996) 165-179.
- [15] J.F. Manwell, J.G. McGowan, E.I. Baring-Gould and W.M. Stein, "Recent Progress in Battery Models for Hybrid Wind Power Systems", in Proc 1995 AWEA Annual Conference.
- [16] Gilbert M.Masters, "Renewable and Efficient Electric Power System", the Solar resource Energy (2004).
- [17] Classic 2 OPzS 190 2v Solar Liquid Cell Technical Data Sheet. 2006.
- [18] Trina Solar, PV module TSM-DC05A.08 Technical Data Sheet. 2014.